Environmental and climate reconstruction of the late-glacial-Holocene transition from a lake sediment sequence in Aubrac, French Massif Central: Chironomid and diatom evidence

Emmanuel Gandouin, Patrick Rioual, Christine Paillès, Stephen J. Brooks, Philippe Ponel, F. Guiter, Morteza Djamali, H. John B. Birks, Valérie Andrieu-Ponel, Michelle Leydet, et al.

Environmental and climate reconstruction of the late-glacial-Holocene transition from a lake sediment sequence in Aubrac, French Massif Central: Chironomid and diatom evidence

E. Gandouin [a,*], P. Rioual [b], C. Pailles [c], S.J. Brooks [d], P. Ponel [a], F. Guiter [a], M. Djamali [a], V. Andrieu-Ponel [a], H.J.B. Birks [e,h], M. Leydet [a], D. Belkacem [a], J.N. Haas [f], N. Van der Putten [g], J.L. de Beaulieu [a]

[a] Aix Marseille Univ, Avignon Univ, CNRS, IRD, IMBE, Technopôle Arbois Méditerranée, Bât. Villemin - BP 80, F-13545 Aix-en-Provence Cedex 04, France
[b] Key Laboratory of Cenozoic Geology and Environment, Institute of Geology and Geophysics, Chinese Academy of Sciences, P.O. Box 9825, 100 029 Beijing, China
[c] Aix Marseille Univ, CNRS, Centre Européen de Recherche et d'Enseignement des Géosciences de l'Environnement, Technopôle Arbois Méditerranée - BP 80, 13545 Aix-en-Provence Cedex 04, France
[d] Department of Life Sciences, Natural History Museum, Cromwell Road, London SW7 5BD, United Kingdom
[e] Department of Biology and Bjerknes Centre for Climate Research, University of Bergen, PO Box 7803, N-5020 Bergen, Norway
[f] University of Innsbruck, Institute of Botany, Sternwartestraße 15, A-6020 Innsbruck, Austria
[g] Lund University, Faculty of Science, Box 118, SE -22100 Lund, Sweden
[h] Environmental Change Research Centre, University College London, London WC1E 6BT, United Kingdom

ARTICLE INFO

Article history:
Received 21 January 2016
Received in revised form 24 August 2016 Accepted 30 August 2016

Keywords:
Western Europe
Past aquatic ecosystem
Temperature reconstruction
Palaeolimnology
Corynocera ambigua
Subfossil insects

ABSTRACT

The analysis of fossil chironomid and diatom assemblages from a sedimentary record from *Les Roustières* peat bog (Massif Central, France, 1196 m asl) allows the reconstruction of past environmental and climate changes during the late-glacial and early Holocene. Chironomid assemblages showed that the infilling of the palaeolake had commenced during the Oldest Dryas (GS-2b) as suggested by the rapid decrease in chironomid species associated with the cold and deep zone of lakes and by their replacement by littoral and eutrophic taxa. Quantitative July temperature reconstructions, based on the chironomid data, suggest that mean July air temperature (Tjul) ranged between 6 °C and 11 °C at the termination of the Oldest Dryas period (GS-2b). Climate began to warm at the start of the Bølling period (GI-1e), between 15,000 and 14,800 cal yr BP, with a rise in Tjul of about 4 °C. This climate warming is contemporaneous with lake eutrophication as suggested by diatoms and chironomids. Maximum temperatures of 13–14 °C were reached around 13,600 cal yr BP during the Allerød period (GI-1c–GI-1a). The Younger Dryas period (GS-1) is marked by a return to cold conditions with Tjul of about 10 °C during a first phase, then 13 °C in its terminal part. A probable increase in the duration of the ice-cover may have favoured arctic and alpine diatom species. The early-Holocene climate improvement is marked by a rise in Tjul of about 3 °C.

1. Introduction

Many palaeoecological studies have focussed on the reconstruction of the palaeoenvironmental and palaeoclimatic conditions that occurred over the late-glacial–early-Holocene transition over Europe, especially in central and northern Europe (Brooks and Langdon, 2014; Coope and Lemdahl, 1995; Lotter et al., 2012). This period is one of the most important for understanding the global mechanisms, such as hydro-climatic changes, that led to the present configuration of European ecosystems. At present, quantitative climate data are available for the late-glacial period at numerous locations (e.g., Brooks and Langdon, 2014; Heiri et al., 2014), such as Britain (Bedford et al., 2004; Lang et al., 2010), Ireland (Watson et al., 2010), The Netherlands (Heiri et al., 2007a), the Swiss Alps (Ilyashuk et al., 2009; Larocque-Tobler et al., 2010), and the Italian Alps (Heiri et al., 2007b; Larocque and Finsinger, 2008). However, to our knowledge relatively few quantitative data have been published from France, and include data from the French Pyrenees (Millet et al., 2012), Jura (Heiri and Millet, 2005), and the Massif Central (Ponel and Coope, 1990). Heiri et al. (2014), based on a review of thirty chironomid-inferred temperature records across Europe, conclude that along the North Atlantic seaboard south of 65°N, enhanced North Atlantic overturning circulation led to warmer temperatures early in the late-glacial interstadial, whereas farther away from the Atlantic, summer temperatures followed the long-term summer insolation trend.

* Corresponding author.
E-mail addresses: emmanuel.gandouin@imbe.fr (E. Gandouin), prioual@mail.igcas.ac.cn (P. Rioual), pailles@cerege.fr (C. Pailles), S.Brooks@nhm.ac.uk (S.J. Brooks), john.birks@uib.no (H.J.B. Birks), Jean-Nicolas.Haas@uibk.ac.at (J.N. Haas), nathalie.van_der_putten@geol.lu.se (N. Van der Putten).

http://dx.doi.org/10.1016/j.palaeo.2016.08.039 0

In the Massif Central, Ponel and Coope (1990) used fossil Coleoptera to characterize the late-glacial interstadial climate warming that occurred around 13,000 uncalibrated years BP, when summer temperatures, according to the Mutual Climate Range method (MCR), were close to present values. According to Ponel and Coope (1990), Allerød summers were colder than during the Bølling. This implies a probable regional climate pattern close to the one observed in Britain and the north-western Atlantic area. This hypothesis is based on only one record and has not been regionally corroborated. Modern techniques of investigation, with better sampling resolution and more precise temperature estimates than are possible with the coleopteran-MCR approach can improve upon the pioneering work from La Taphanel (Ponel and Coope, 1990). In particular, chironomid analysis is a useful technique because i) chitinous remains of chironomids are generally abundant in freshwater sediments and ii) chironomid-based inference models for summer temperature have low root mean squared error of prediction (RMSEP) (e.g. 1.40 °C in Heiri et al., 2011).

Chironomids have been widely used as indicators of past changes in lake-water quality since a classification of lake trophic types was established by Brundin (1958). Some studies have shown that chironomids can be used to reconstruct total phosphorus (Brooks et al., 2001) and chlorophyll *a* concentrations (Brodersen and Lindegaard, 1999). Chironomids are also sensitive to many other environmental variables such as pH (Mousavi, 2002), dissolved oxygen concentration (e.g. Quinlan and Smol, 2001), salinity (Henrichs et al., 2001), the nature of the substratum (e.g. Larocque et al., 2001) and lake-water depth (Chen et al., 2013). According to Juggins (2013), however, some of these variables can co-vary with climate factors and can cause problems for chironomid-based reconstructions of past climate. Juggins (2013) encourages palaeoecologists to be more critical of their models and reconstructions. Multiproxy studies are probably one of the best ways to estimate the bias of quantitative climate reconstructions, because it is easier to disentangle local events from regional ones. Because diatoms are very good indicators of changes in limnological conditions (Stoermer and Smol, 1999), their combination with chironomids can lead to useful reconstructions of past aquatic ecosystems. Such a study has already been presented by Larocque and Bigler (2004) for a high-elevation lake in Sweden. In this study, diatoms are used to identify limnological changes (in water chemistry, lake-level) that may interfere with the chironomid-based climate reconstruction.

The Aubrac Mountain is rich in potential palaeoecological sites such as mountain lakes and peat bog sediments. Beaulieu et al. (1985) explored in detail the past vegetation of this part of the Massif Central since the late-glacial, with however a poor radiocarbon chronological control. One of their key sites, which they named *Brameloup*, has a long sedimentary record and a high sedimentation rate and is therefore particularly suitable for a new multidisciplinary study including pollen, Coleoptera, plant macro-fossil, diatom, and chironomid analyses.

The present paper focuses on aquatic ecosystem proxies, specifically chironomid and diatom subfossils from the *Brameloup* (renamed here *Les Roustières*) record. The palaeobotanical and Coleoptera data will be published elsewhere and only a preliminary pollen diagram is presented here in order to help place our radiocarbon chronology into the regional bio-chrono-stratigraphy (cf., Beaulieu et al., 1985).

Our main goal here is to provide an original quantitative reconstruction of mean July air temperature (Tjul) and to determine if any abrupt climate changes are regionally recorded by the aquatic communities. In this case, what are the magnitudes of these events? Is the climate pattern in the Massif Central similar to that observed in the north-western Atlantic area or is it belong to the same climate configuration of more continental site?

2. Study area

The site (44° 42′ 42″N; 3° 5′ 17″E, 1196 m asl) is located in the French Massif Central (Fig. 1), on the Aubrac plateau, which extends over 38,000 ha between the north-western volcanic Cantal massif and the south-eastern "Causse de Sauveterre" area. A steep slope marks the limit between the Aubrac summits (1471 m) and the Causse. To the north, the Aubrac plateau gently turns towards the Truyère valley, with elevations ranging between 1200 m and 1000 m.

The bedrock is composed of metamorphic and granitic rocks, mainly covered by a basaltic layer (Ayral, 1928) formed during the Villafranchian eruptive episode (Colin, 1966). On these two substrata are scattered abundant and sometimes thick glacial and periglacial deposits, attributed by Poizat and Rousset (1975) to three episodes of glaciation, covering about 30,000 ha. Glacial erosion or morainic accumulations created numerous closed depressions now occupied by lakes or peat bogs. Hence, numerous wetlands are located on the Aubrac plateau and help to make this region an area of great ecological value. Many floristic and faunal glacial relict species such as *Vipera berus* and *Notaris aethiops* (Coleoptera, Curculionidae) still inhabit this region today and their presence is interpreted as being related to extreme climate conditions (Nozeran, 1953). Because of frequent temperature inversion episodes due to the superposition of a cold, heavy and stagnant northern air mass with a warm, lighter and more mobile southern current (Mediterranean influence), especially in winter (Gachon, 1946), mean annual temperatures are 5 °C lower than anywhere else in France at comparable elevations. The modern average temperatures of the warmest month are about 20–25 °C and −5–0 °C for the coldest month (Météo France, 2003). Kessler and Chambraud (1986) report for the Mende station (730 m) an average of 25 °C for July maximum temperature. Using a lapse rate of 0.6 °C/100 m, a July mean temperature of 22.6 °C can be extrapolated for our study site. Rainfall mainly comes from the Atlantic Ocean and ranges between 1000 mm yr^{-1} on the plateau to 1400 mm yr^{-1} on the west-facing upper ridges.

The major part of the Aubrac is located within the mountainous region near the ecotone between the forest and alpine zones. The potential natural vegetation is a mountain beech (*Fagus sylvatica*) forest, which is still abundant to the west but mixed with Scots pine (*Pinus sylvestris*) to the north-east. It is, however, reduced to small thickets on most of the plateau due to human activities. The Aubrac plateau is characterized by its open landscape with large meadows enclosed inside long walls made of basaltic stones and used for cattle breeding, and heath dominated by *Calluna vulgaris* or *Cytisus purgans*.

Les Roustières peat bog (Fig. 1) lies within a glacial corrie of about 25 ha which was completely filled in during the Holocene (Beaulieu et al., 1985). The peat bog is upstream of *Les Roustières* brook. La Taphanel (975 m asl), studied by Ponel and Coope (1990), is located 100 km north of *Les Roustières* (1196 m).

3. Methods

3.1. Coring, radiocarbon dating, and age-depth model

Les Roustières peat bog was sampled with a Russian peat corer, allowing ten successive core sections of 1-m long and 7-cm wide to be obtained. A 10 m core profile was retrieved from the centre of the bog, where the late-glacial deposits were known to be thickest (Beaulieu et al., 1985).

Twenty-two sediment samples were dated using the conventional radiocarbon method at the Poznan (Poland) and Gif sur Yvette (France) Radiocarbon Laboratories (Table 1). The nature of the substratum close to the lake is mainly basaltic and granitic (Ayral, 1928), which minimizes the risk of contamination by carbonates and allows us to do bulk dates. The dates were calibrated using the CLAM software (Blaauw, 2010) associated with the statistical software R (version 3.0.1) (Core Team, 2012) and the non-marine (IntCal13) radiocarbon calibration (Reimer et al., 2013). The dates are calculated at 2 standard deviations. The age-depth model was developed using the smooth spline method (spar = 0.3 and 10,000 iterations) between dated levels

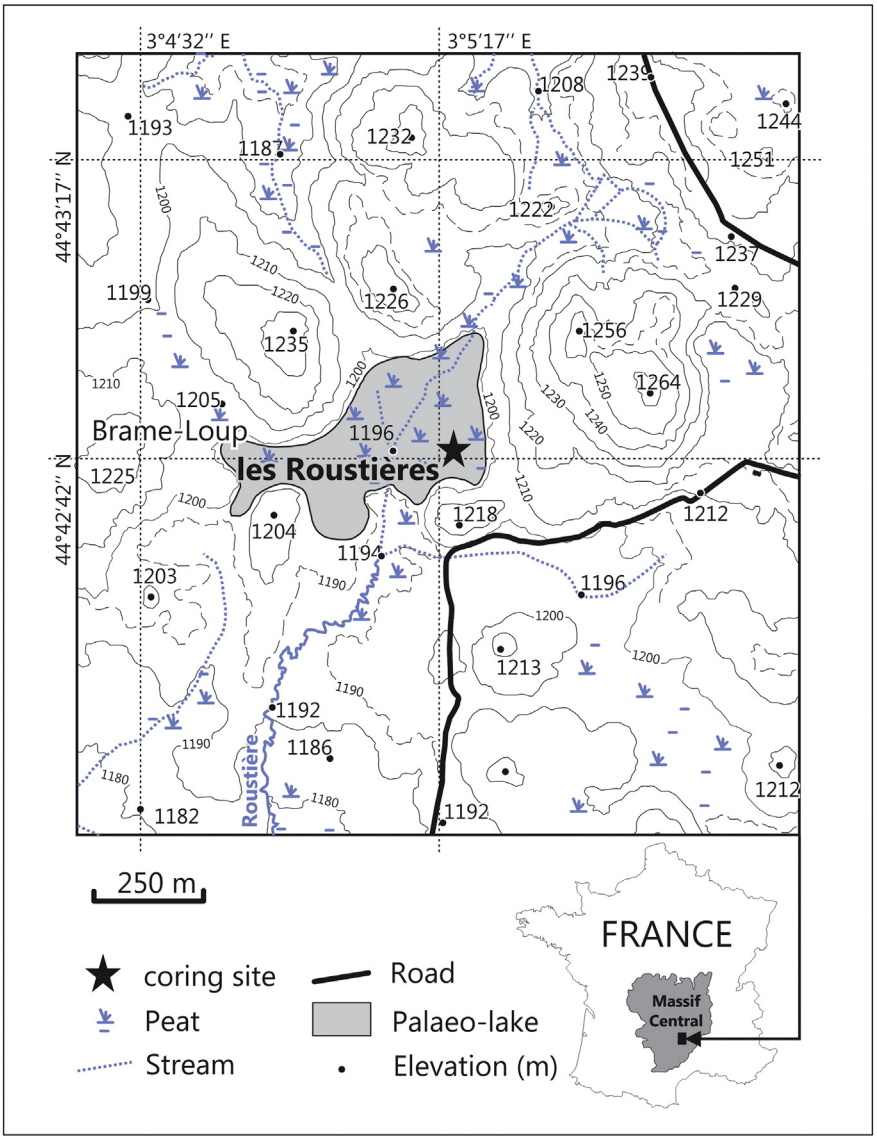

Fig. 1. Location of the study area.

with the same software. In order to plot proxy values against calendar age, CLAM software returns a single 'best' age-depth model (cf., Blaauw, 2010).

3.2. Chironomid analysis

Forty-seven sediment samples, weighing between 9 and 21 g, with a thickness of 1 cm, were analysed from depths between 600 and 1000 cm, at a minimum of 5 cm intervals; which corresponds to an average temporal resolution of about 150 years (min = 140 years in late-glacial gyttja; max = 180 years in Oldest Dryas clay). Laboratory methods for the extraction of the chironomid remains consisted of successive treatments of KOH (10%; 70 °C), to de-flocculate the sediment, and water-washing over a 100 μm sieve (Hofmann, 1986), combined with paraffin flotation (Coope, 1986). A minimum of 50 head capsules per sample must be picked out in order to provide realistic estimates of environmental conditions (Heiri and Lotter, 2001; Larocque, 2001). Head capsules that included at least half the mentum were counted. The larval head capsules were identified with reference to Klink and Moller Pillot (2003), Rieradevall and Brooks (2001), Schmid (1993), Wiederholm (1983) and Brooks et al. (2007). The relative abundance of each chironomid taxon for each sample is presented as a stratigraphical diagram using the TILIA and TILIA-GRAPH software (Grimm, 1991).

3.3. Chironomid–temperature transfer function

Mean July temperature estimates were made using a weighted-averaging partial least squared (WA-PLS), 2-component, chironomid-based mean July air temperature inference model. The fossil data were square-root transformed, and the C2 program was used (Juggins, 2010). This inference model is based on a modern calibration set of 274 lakes from Norway and Switzerland, including 151 chironomid taxa, spanning a mean July air temperature range of 3.5–18.4 °C, and has a root mean squared error of prediction of 1.40 °C and a bootstrapped r^2 of 0.87 based on leave-one-out cross-validation (Heiri et al., 2011). Because of the dominance of both *Corynocera ambigua* and unresolved Tanytarsini, the statistical significance of the temperature reconstruction has been tested using the Telford and Birks (2011) test. According to this test, the proportion of variance in the fossil data explained by the reconstruction is estimated using constrained ordination. Then, using the biological data from the same training-set, a large number of reconstructions are made using transfer functions trained on random environmental variables. The proportions of the variance

Table 1
Radiocarbon dates from *Les Roustières* peat bog, calibrated with the CLAM software (Blaauw, 2010) associated with the statistical software R (version 3.0.1) (R Core Team, 2012) and the non-marine (IntCal13) radiocarbon calibration (Reimer et al., 2013). The dates in italics are considered too young according to the regional pollen-based chronology for the late-glacial interstadial in the Aubrac Mountain (Beaulieu et al., 1985) and are treated as outliers in the age model.

Lab-code	Depth	Nature	mg C	$\delta^{13}C$	pMC	Radiocarbon yr BP	Calibrated BP and (cal.min cal.max probability)
Poz-16151	600–601	Peaty gyttja	4.23	−26	33.44 ± 0.19	8799 ± 45	9610–9616 (0.5) 9626–9964 (73.4) 9984–10,153 (21.1)
SacA 10451	607–608	Gyttja	1.2	−24.5	33.57	8770 ± 30	9634–9642 (0.9) 9660–9906 (94.1)
SacA 10452	*615–618*	*Gyttja*	*1.07*	*−24.8*	*34.25 ± 0.14*	*8605 ± 30*	*9526–9628 (95)*
SacA 10453	620–622	Gyttja	1.07	−23.2	33.32 ± 0.14	8830 ± 35	9706–9719 (1.5) 9733–9958 (63.8) 9987–10,042 (8.4) 10,057–10,150 (21.5)
SacA 10454	*637–640*	Gyttja	*1*	*−23.5*	*33.49 ± 0.14*	*8785 ± 35*	*9633–9642 (0.6)* *9659–9922 (91.9)* *10,078–10,114 (2.5)*
SacA 10455	650–653	Gyttja	1.4	−23.2	31.01 ± 0.13	9405 ± 35	10,557–10,731 (95)
SacA 10456	660–664	Gyttja	1.56	−22.8	30.32 ± 0.16	9585 ± 45	10,745–11,128 (95)
SacA 10457	680–681	Gyttja	0.98	−22	29.88 ± 0.13	9705 ± 35	10,888–10,923 (5.3) 11,087–11,218 (89.6)
SacA 10458	690–692	Gyttja	1.18	−20	30.22 ± 0.13	9615 ± 35	10,782–11,035 (68.1) 11,060–11,166 (26.9)
SacA 10459	715–720	Gyttja	1.44	−20.7	28.48 ± 0.13	10,090 ± 35	11,404–11,459 (5.9) 11,461–11,569 (14) 11,592–11,826 (70.4) 11,884–11,906 (1.5) 11,918–11,957 (3.1)
Poz-16152	730–735	Clayey gyttja	1.62	−19.6	28.08 ± 0.19	10,202 ± 54	11,628–11,653 (2.6) 11,696–12,108 (92.4)
SacA 10460	745–750	Clayey gyttja	1.51	−19.7	26.6 ± 0.13	10,635 ± 40	12,446–12,455 (0.9) 12,534–12,682 (94.1)
Poz-16155	755–760	Clayey gyttja	2.98	−18.8	25.59 ± 0.17	10,948 ± 53	12,648–12,980 (91) 13,014–13,063 (3.9)
SacA 10461	760–765	Gyttja	1.59	−19.8	25.54 ± 0.13	10,965 ± 40	12,657–12,973 (93.3) 13,028–13,054 (1.7)
SacA 10463	*810–815*	*Gyttja*	*1.49*	*−19.3*	*28.01 ± 0.13*	*10,225 ± 40*	*11,769–11,790 (2.3)* *11,803–12,086 (92.6)*
SacA 10464	820–825	Gyttja	1.28	−23.5	24.83 ± 0.12	11,190 ± 40	12,902–13,234 (95)
Poz-16154	*835–840*	*Gyttja*	*2.54*	*−22.3*	*25.35 ± 0.17*	*11,024 ± 53*	*12,705–13,092 (95)*
SacA 10465	855–860	Gyttja	1.48	−20.1	23.81 ± 0.12	11,530 ± 40	13,268–13,477 (95)
SacA 10466	870–875	Gyttja	1.45	−22.6	22.2 ± 0.12	12,090 ± 45	13,789–14,081 (95)
Poz-16153	885–891	Gyttja	2.42	−18.1	20.29 ± 0.14	12,812 ± 55	14,909–15,669 (93.2) 15,751–15,841 (1.7)
SacA 10468	930–935	Clay	1.01	−20.8	17.95 ± 0.12	13,800 ± 50	16,742–17,075 (95)
SacA 10469	970–975	Clay	0.68	−19.2	16.74 ± 0.11	14,360 ± 50	17,148–17,803 (95)

explained by these random reconstructions are estimated. If the reconstruction of interest explains more of the variance than 95% of the random reconstructions, the reconstruction is deemed statistically significant at $p < 0.05$.In order to complete the reconstruction diagnostic statistics, goodness-of-fit to temperature was evaluated by passively positioning the fossil samples on a CCA of the modern training set constrained solely against July temperature. Any fossil samples that had a squared residual distance value within the most extreme 10% of values in the modern training set were considered to have a poor fit-to-temperature (very poor fit for 5%). The modern analogue technique (MAT) was used to detect fossil samples that lacked good analogues in the modern calibration dataset using squared chord distance as a measure of dissimilarity. Samples with a dissimilarity larger than the 95% threshold in the modern data were considered as having no good analogues in the modern calibration data set (Birks et al., 1990; Birks, 1995, 1998; Velle et al., 2005).

3.4. Diatom analysis

The section between 600 and 1000 cm was analysed to provide an insight into the dynamics of the diatom assemblages in the late-glacial and early Holocene. Diatom samples (1 cm thick) were taken at 8, 5, 4, or 1 cm intervals. In total, 66 samples were analysed.

Sediment samples were prepared using a hot mixture of H_2O_2:H_2O followed by a rinse and decanting in distilled water. Diatom concentration was estimated using the microsphere method developed by Battarbee and Kneen (1982) and expressed as number of valves per milligram of dry sediment (valves·mg^{-1}). Sub-samples of the homogenized solution were then diluted by adding distilled water and left to settle onto coverslips until dry. The coverslips were fixed onto glass slides with Naphrax (mountant with a refraction index of 1.73). Counting was done using a Nikon NS600 microscope at ×1000 magnification. The total number of valves counted per sample varied from 50 (sub-sterile samples) to >1000 (rich samples). For rich samples, counting stopped when no new species were encountered after 2 transects of the slides. Diatom identification and taxonomy are mainly based on Krammer and Lange-Bertalot (1986, 1988, 1991a, 1991b) but with current diatom nomenclature. Chrysophyte cysts were counted but morphotypes were not identified. The ratio of diatom frustules (=2 valves) to chrysophyte cysts (D:C ratio) was calculated to show the relative proportion between these two algal groups. This ratio is a simple way of estimating trends in algal succession and can help to refine palaeoecological interpretations (Smol, 1985). The computer

program C2 (version 1.6.5, Juggins, 2010) was used for drawing the stratigraphical diagram.

3.5. Statistical analyses of the biological sub-fossil data

Chironomid and diatom assemblage zones (RCh- and RDaz-) were determined using optimal sum-of-squares partitioning (Birks and Gordon, 1985) using the software ZONE (Lotter and Juggins, 1991). The number of significant zones was determined by the "broken-stick" model (Bennett, 1996) using the BSTICK software (Birks and Line, unpublished software).

Detrended Correspondence Analysis (DCA) was performed on the chironomid and diatom data that were square-root transformed in order to stabilize variances. Taxa with only one occurrence within the data-set were removed from the numerical analyses. The DCA was carried out with detrending by segments and down-weighting of rare species using CANOCO version 4.5 (ter Braak and Šmilauer, 2002).

To compare the species richness of the diatom fossil samples, counts were standardized using rarefaction analysis. This numerical technique provides an estimate of species richness for samples of different sizes (Birks and Line, 1992). The richness measure derived from rarefaction analysis is called the expected species richness, E(Sn), the number of taxa found if all the sample counts were the same size. This is the simplest and most interpretable richness parameter available for palaeoecological data. Rarefaction analysis was performed using the program PAST (Hammer et al., 2001) using a common count sum of 300. $E(S_{300})$ was not calculated for samples 921, 890, and 601 cm as their count sums were too low (<70).

4. Results

4.1. Lithostratigraphy, radiocarbon dating, and pollen stratigraphy

The lithostratigraphical sequence (Fig. 2) comprises a succession of clays and organic gyttja from 1000 to 600 cm. From the basal part to about 900 cm, the sediment is mainly minerogenic (clay). This suggests low lake productivity and large erosive processes in the watershed. After 900 cm, the sediment becomes biogenic with algal gyttja and without any detrital coarse input. This suggests an increase in lake productivity. Between 783 and 734 cm, clay reappears, probably due to a fall in lake productivity possibly associated with major climate cooling (such as the Younger Dryas Event). Sediments are then composed of gyttja until 605 cm, where a peat layer begins, probably due to the natural infilling of the basin.

The radiocarbon dates provided a chronology from the late-glacial to the early Holocene (Table 1). The sediment sample "Sac A 10467" did not provide any date because of insufficient carbon for dating. The samples "Sac A 10452", "Sac A 10454", "Sac A 10463" and "Rous_3" were identified as outliers. Considering the age-model (Fig. 2) and the pollen stratigraphy (Fig. 3) we achieved an approximately decadal to centennial resolution for the two biological records from the Oldest Dryas (Gs2-b) to the early Holocene period.

A rise in sedimentation rate at ca 13,000 cal BP is particularly striking since about one meter of gyttja has been deposited in ca 4 and 7 centuries (according to the age-depth model intervals at 2 sigmas). As mentioned above, this section is marked by biogenic sedimentation without any detrital coarse input. Therefore, this episode of rapid accumulation was not due to any erosion process but could be linked to an increase of lake productivity.

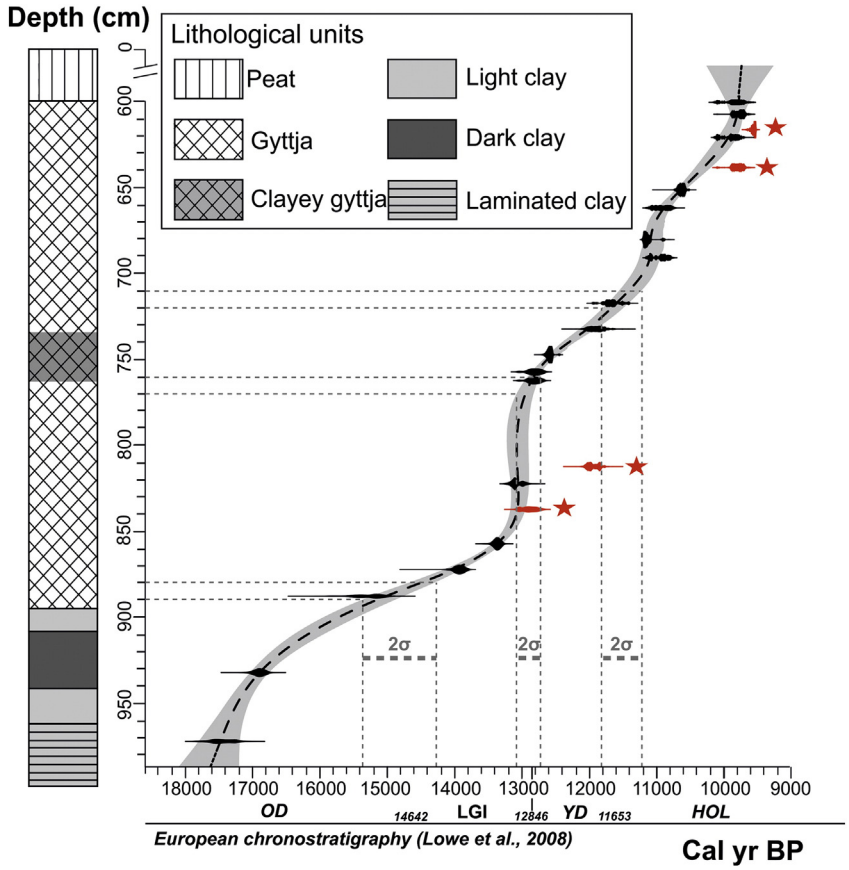

Fig. 2. Radiocarbon age-depth model developed with the CLAM software (Blaauw, 2010) using a smooth spline method with 10,000 iterations and the "IntCal13" ^{14}C calibration curve. The dates marked by a star are considered as outliers. Boundaries between the Older Dryas (OD), late-glacial interstadial (LGI), Younger Dryas (YD), and Holocene (HOL) are shown as dotted grey lines with 2 standard deviations (2σ).

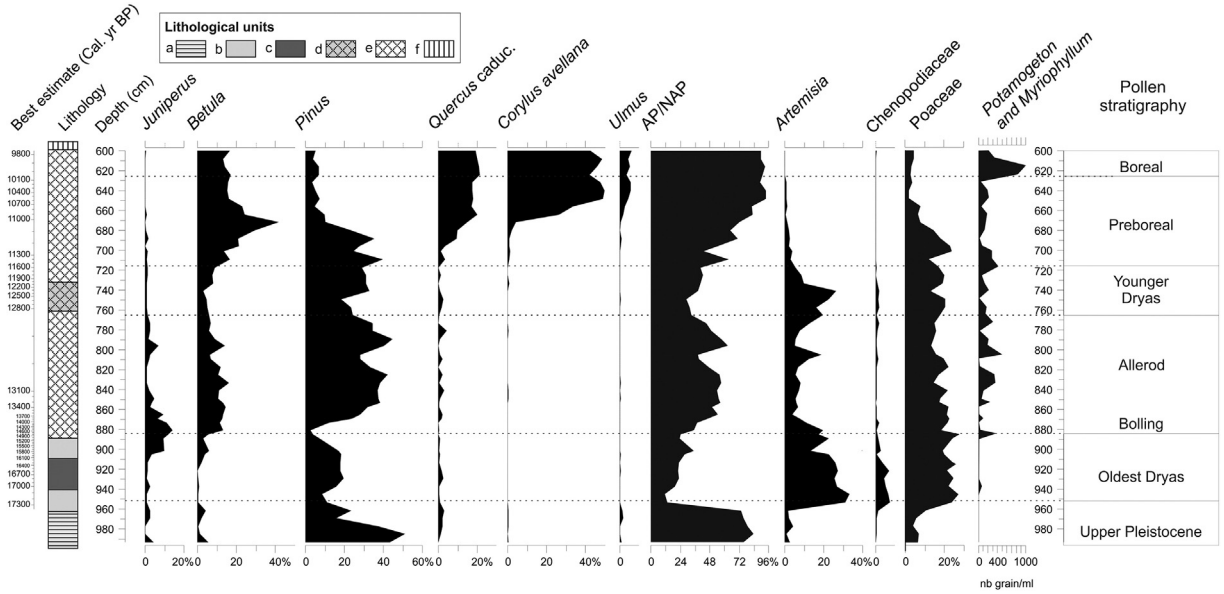

Fig. 3. Simplified pollen diagram and lithological column from *Les Roustières*. a: laminated clay; b: light clay; c: dark clay; d: clayey gyttja; e: gyttja; f: peat.

Based on pollen data from *Les Roustières* (Fig. 3) and following the regional pollen stratigraphy established by Beaulieu et al. (1985), we propose to fix (i) the onset of the late-glacial interstadial (LGI) (Bølling-Allerød) at between 890 and 880 cm (15,371–14,298 cal yr BP $\pm$ 2σ) with the rise in *Betula* and *Pinus* percentages and decrease in *Artemisa*; (ii) the LGI–YD boundary between 770 and 760 cm (13,080–12,734 cal yr BP $\pm$ 2σ) with the rise in *Artemisia* and decrease in *Pinus* percentages; and (iii) the onset of the Holocene interglacial between 720 and 710 cm (11,797–11,229 cal yr BP $\pm$ 2σ) with the rise in both *Betula* and *Pinus* percentages and the start of the continuous curves of deciduous *Quercus* and *Corylus avellana*. The present pollen stratigraphy related to the age-model established at *Les Roustières* matches with the European chronostratigraphy proposed by Lowe et al. (2008) with only very few discrepancies that can be related to methodological biases as associated with sample thickness, sample resolution, and the classical radiocarbon error range.

4.2. Chironomids

Sediment from 993 to 958 cm contained no chironomid head capsules. This may be explained by the climatic and environmental conditions that prevailed during the glacial period, which may have been too harsh for the occurrence of chironomids. Altogether 54 taxa were identified from the 41 levels sampled from 957 to 600 cm. A mean number of 106.5 head capsules per sample were counted (nmin = 47 capsules at 945 cm, nmax = 243 at 700 cm), totaling 4369 head capsules. The core sequence analysed was partitioned (following the "broken-stick" model) into four chironomid assemblage zones: RCh1 to RCh4 (Fig. 4).

After removal of rare taxa, DCA (Fig. 4 and Supplementary Table 2) was performed on the 33 taxa in 41 samples totalling 4148 head capsules (95% of the whole dataset). DCA axes 1 and 2 have, respectively, eigenvalues of 0.34 and 0.09. The DCA-axis 1 gradient length is about 3 standard deviation (SD) units. The first DCA axis is associated with both temperature and lake-level gradients related to both climate warming and the natural infilling of the lake as suggested by a fauna typical of the cold profundal zone of oligotrophic to mesotrophic lakes such as *Stictochironomus* (Wiederholm, 1983; Lotter et al., 1997; Brooks et al., 2007), *Protanypus* (Walker and MacDonald, 1995), *Sergentia coracina* (Brodin, 1986; Brooks et al., 2007), and *Paracladius* (Brooks et al., 2007) contrasting with a more littoral fauna of mesotrophic to eutrophic warmer lakes with *Parakiefferiella bathophila* group (Hofmann, 1984), *Parachironomus arcuatus* group (Buskens, 1987; Brodersen et al., 2001), *Chironomus* spp. (Brooks et al., 2007), *Endochironomus* spp. (Cranston, 2010), and *Corynoneura scutellata* group (Moller Pillot and Buskens, 1990). The second DCA axis is difficult to interpret because of the regrouping of both oligotrophic lacustrine taxa such as *Tanytarsus lugens* group (Brundin, 1956; Brodin, 1986) and *Pagastiella orophila* (Brooks et al., 2007) with the eutrophic lacustrine taxon *Polypedilum* spp. (Brooks et al., 2007). This assemblage is opposed to rheophilous taxa such as *Eukiefferiella/Tvetenia* (Wiederholm, 1983; Brooks et al., 2007) and other taxa associated with macrophytes such as *Paratanytarsus* spp. (Buskens, 1987; Brodersen et al., 2001), *Corynoneura scutellata* group (Kesler, 1981), and *Cricotopus sylvestris* group (Brodersen et al., 2001).

4.2.1. Zone RCh1: samples 957 to 945 cm (17,315 to 17,145 cal yr BP, best estimate)

Chironomid assemblages from RCh1 are characterized by the dominance of *Stictochironomus* and high percentages of *Stempellinella/Zavrelia*, *Paracladius*, *Protanypus*, and *Corynocera ambigua*. The *Stempellinella/Zavrelia* group covers a wide range of ecological conditions from oligotrophic to eutrophic lakes and streams (Brooks et al., 2007; Wiederholm, 1983). *Stictochironomus* inhabits deep soft sediment or littoral sand of oligotrophic to mesotrophic lakes (Wiederholm, 1983). Korhola et al. (2002) consider it as cold stenothermous since this taxon preferentially colonizes arctic habitats (Danks, 1981). In NW Europe (Norway and Spitzbergen), *Stictochironomus* reaches a maximum abundance in lakes with Tjul air temperatures ranging from 8 to 14 °C (Brooks and Birks, 2000). In the Swiss Alps it occurs in lakes up to an elevation of 1500 m (Lotter et al., 1997), with Tjul air temperatures ranging from 7.9 °C to 11.7 °C.

Quinlan and Smol (2001) consider the genus *Paracladius* to be indicative of highly oxygenated water. This genus can be considered as cold stenothermous, since it occurs in Swiss alpine lakes up to 1500 m (Lotter et al., 1997) in which Tjul air temperatures range from 7.6 °C to 10.7 °C.

Protanypus is also an indicator of highly oxygenated water (Quinlan and Smol, 2001) and colonizes cold (Olander et al., 1999) and oligotrophic lakes (Wiederholm, 1983), preferring deep zones (Brooks and Birks, 2000). At present, this genus has its maximum occurrence at a July temperature ranging from 6 to 10 °C in Swiss lakes (Heiri and Millet, 2005).

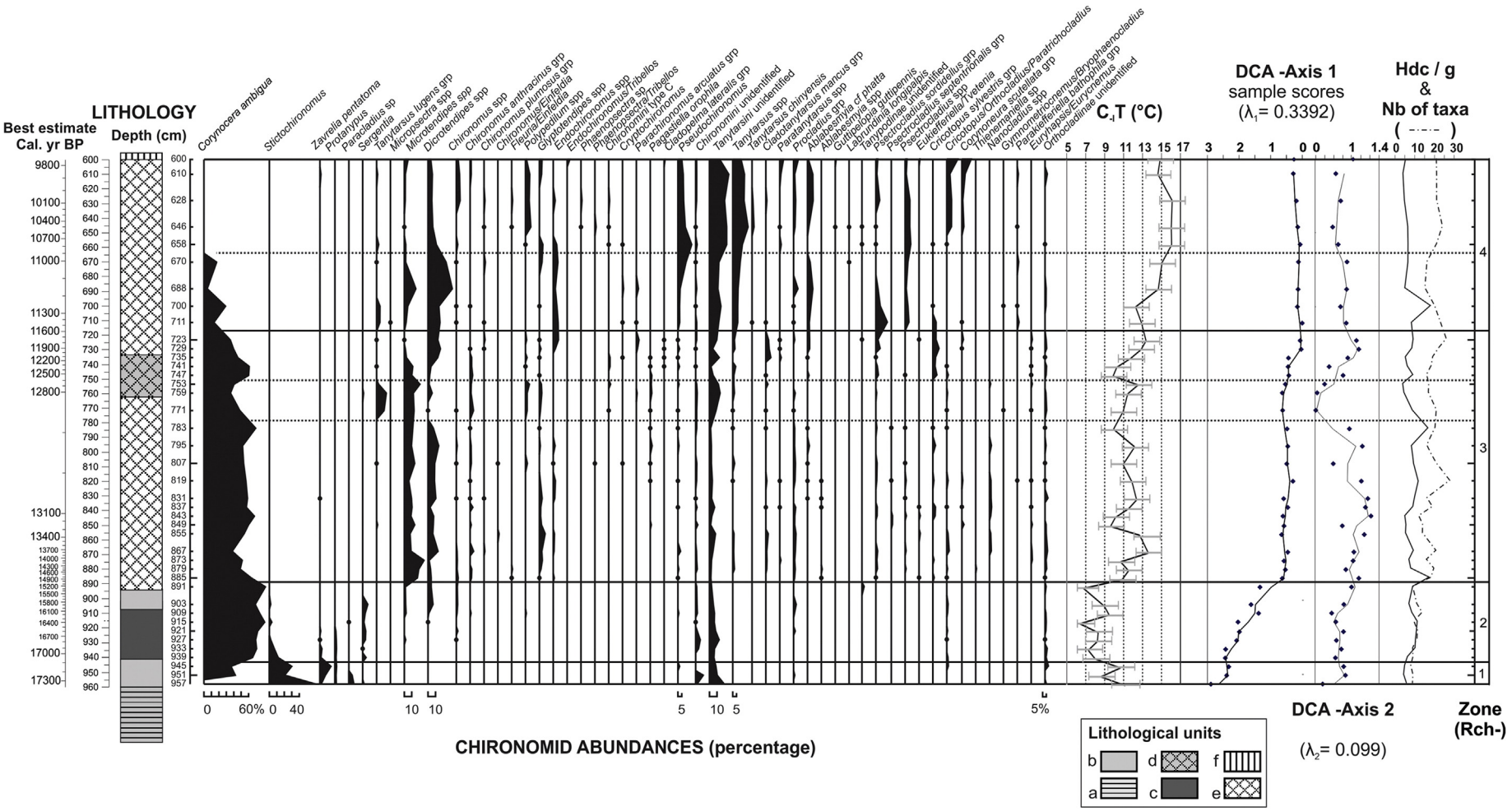

Fig. 4. Summary diagram showing selected chironomid taxa encountered in *Les Roustières* sediments (%). The diagram zonation was determined using optimal sum of square partitioning (Birks and Gordon, 1985) using the software ZONE (Lotter and Juggins, 1991). The number of significant zones was determined by the "broken-stick" model using the BSTICK software (Birks and Line, unpublished). The statistically significant zones are delimited by solid lines. The dotted lines delimit the non-significant zone established by a constrained sum-of-squares cluster analysis (CONISS: Grimm, 1987). The names of lithological units (a–f) are given in Fig. 3.

Corynocera ambigua has a wide modern geographical distribution ranging from northern to central Europe but is presently absent in France. The cold stenothermous character of *C. ambigua* has been questioned by Brodersen and Lindegaard (1999) who have shown mass occurrences of this species in warm water in Danish lakes (around 20 °C). These authors show that *C. ambigua* expansion is facilitated in clear waters, rich in benthic diatoms and with abundant aquatic vegetation (such as charophytes). *C. ambigua* is broadly distributed along an elevational gradient in the subarctic region of northern Sweden (Larocque et al., 2001). In their dataset, the Tjul optimum of this taxon is 10.4 °C, which is relatively low for French latitudes. Larocque and Hall (2004) argue that there is no simple relationship between temperature, depth, and the occurrence of *C. ambigua*. This seems to be confirmed by Barley et al. (2006), who show that the distribution and abundance of *C. ambigua* is not correlated with temperature but it is often abundant in shallow lakes in a north-west North American dataset where *C. ambigua* preferentially occurs in shallow lakes <4 m deep.

In summary, the chironomid fauna from zone RCh1 is characteristic of an oligotrophic lake with highly oxygenated waters in cold climatic conditions. The radiocarbon dates suggest this is towards the end of the Oldest Dryas. The rapid diminution of profundal taxa such as *Stictochironomus* and *Protanypus* suggests that water depth decreased throughout the zone, which probably facilitated the occurrence of *C. ambigua.*

4.2.2. Zone RCh2: samples 939 to 891 cm (17,040 to 15,210 cal yr BP, best estimate)

This zone is marked by the maximum abundance of *C. ambigua* (up to 90%), a decrease and almost disappearance of profundal taxa, such as *Stictochironomus* and *Protanypus,* and the appearance of littoral taxa, such as *Microtendipes* and *Dicrotendipes*, in the upper part of the zone. These taxa are also often associated with dense aquatic vegetation in shallow lakes or with warm summer temperatures (Hofmann, 1984; Brooks, 2006).

RCh2 is also marked by the appearance of *Sergentia*, a genus typical of arctic and alpine lakes with mesotrophic to oligotrophic waters (Lotter et al., 1997; Larocque et al., 2001). Heiri (2004) has shown that *Sergentia* tends to occur at higher abundances in the deepest part of shallow Norwegian lakes. This is also the case in north-west North America (Barley et al., 2006) where *Sergentia* preferentially occurs in lakes deeper than 4 m. The top of the zone is marked by the first occurrence of thermophilic and mesotrophic to eutrophic taxa such as *Chironomus* and *Dicrotendipes* (Brodin, 1986), suggesting that the climate was still cool but was starting to become warmer and that the lake was more nutrient-rich.

4.2.3. Zone RCh3: samples 885 to 723 cm (14,825 to 11,745 cal yr BP, best estimate)

This zone is marked by higher taxonomic richness than in the two previous ones. This indicates the habitat diversification that took place during the late-glacial interstadial climatic improvement. Hence, some thermophilic and mesotrophic to eutrophic taxa such as *Glyptotendipes*, *Endochironomus* (Larocque et al., 2001) and the *Cladotanytarsus mancus* group (Brooks et al., 2007) appear. Abundant taxa such as *Microtendipes*, *Dicrotendipes*, *Glyptotendipes,* and *Ablabesmyia* (e.g., Brooks et al., 2007) are indicators of well-developed macrophytic vegetation around the littoral margins and suggest the prevalence of shallow-water conditions.

Several assemblage fluctuations are recorded in zone RCh3. The onset of the zone is characterized by occurrences of rheophilic genera such as *Eukiefferiella/Tvetenia* (Gandouin et al., 2006) which could be explained by increased runoff from streams. This may be associated with the melting of snow patches in the area in response to regional climate warming. The 771 and 753 cm (12,960 and 12,695 cal yr BP, best estimate) levels are mainly characterized by a decrease in *C. ambigua* percentages and high values of *Tanytarsus lugens* group. This last taxon usually occurs in the deep part of oligotrophic lakes or in the littoral zone of cold subalpine and subarctic lakes (Brodin, 1986). This faunal change may be related to a rise in lake level and/or a climate cooling. The end of RCh3, from 735 to 723 cm *(12,115 to 11,745 cal yr BP, best estimate)* is marked by a large decrease in *C. ambigua* and *Microtendipes* and a rise in several thermophilic taxa such as *Endochironomus* (Larocque and Finsinger, 2008), *Dicrotendipes* and *Cladotanytarsus mancus* group (Brooks et al., 2007), that are likely related to climate warming, probably the onset of the Holocene. Moreover, the continuous percentages of *Ablabesmyia* cf. *phatta*, a taxon associated with acidic conditions (Berezina, 2001) and peat-bog environments, may mark a reduction in the open-water surface of the site by telmatic peat development. Acidic conditions are also favourable to species of *Psectrocladius* (Brooks, 1996), *Cladotanytarsus mancus* group (Brooks et al., 2007), and *Parachironomus arcuatus* (Mousavi, 2002), which also increase from this point in the sequence.

4.2.4. Zone RCh4: samples 711 to 600 cm (11,435 to 9785 cal yr BP, best estimate)

Zone RCh4 is marked by the progressive disappearance of *C. ambigua* coupled with the rise in abundances of several taxa of *Orthocladiinae* (such as *Psectrociadius* genus, *Corynoneura scutellata* and *Cricotopus/Orthocladius/Paratrichocladius* groups) and Chironomini (such as *Glyptotendipes* and *Polypodium*) which are linked to dense macrophytic vegetation (Brodersen et al., 2001; Brooks et al., 2007). RCh4 is also characterized by increasing percentages of thermophilic taxa such as *Dicrotendipes, Pseudochironomus*, and *Chironomus*. In the first part of RCh4, from 711 to 670 cm, littoral taxa such as *Dicrotendipes, Endochironomus,* and *Microtendipes* reach their maximum abundance, which could be related to abundant macrophyte growth in shallow waters. In the terminal part of RCh4, from 658 to 600 cm, *C. ambigua* completely disappears and thermophilic taxa reach maximum abundance, which may indicate that the highest temperatures were reached. The rise in percentages of both *Cricotopus/Orthocladius/Paratrichocladius* and *Corynoneura scutellata* groups may be related to macrophyte development as the *C. scutellata* group is often associated with semi-submerged vegetation (Brooks, 2000) such as *Typha*, where the larvae are grazers on periphyton communities (Kesler, 1981).

4.2.5. Chironomid temperature reconstruction

The Telford and Birks (2011) test indicates that the temperature reconstruction from *Les Roustières* is statistically significant ($p < 0.05$) and suggests that temperature is the major driver of change in the chironomid assemblages. Two thirds of subfossil samples have a 'close' analogue in the modern calibration data set (Fig. 5), but there are samples that have no close analogue in RCh-1 and Rch-4 chironomid zones. Nevertheless, the goodness-of-fit statistics revealed that only 22% of the samples have a 'poor' fit in Rch-4. In the late-glacial, 22% of the samples have a 'poor' fit and 34% have a 'very poor' fit with temperature. All the Younger Dryas samples have a 'good' fit while it is the contrary for the Oldest Dryas. These lack-of-fit measures indicate that the fossil chironomid assemblages in those samples may be responding to changes in an environmental variable other than temperature. Hence the temperature reconstructions from those samples, especially in the Older Dryas where goodness-of-fit values are particularly extreme, may be less reliable and should be considered as tentative and interpreted with caution.

The reconstruction (Fig. 5) reveals several thermal fluctuations. The initial climate warming occurred around 15,000 cal yr BP when Tjul rose from 7 °C to 11 °C. A maximum of about 13.5 °C was reached around 13,800 cal yr BP. A second thermal optimum of 16 °C occurred after 10,800 cal yr BP in the earliest part of the Holocene. The late-glacial interstadial seems to be marked by decreases (−3 °C/−2 °C: from 13/12 to 10/9 °C) in summer temperature around 13,200 cal yr BP and 12,900 cal yr BP. A second climate minimum was reached when chironomid-inferred temperatures reached about 10 °C around 12,600 cal yr BP, in the Younger Dryas period. The end of the Younger

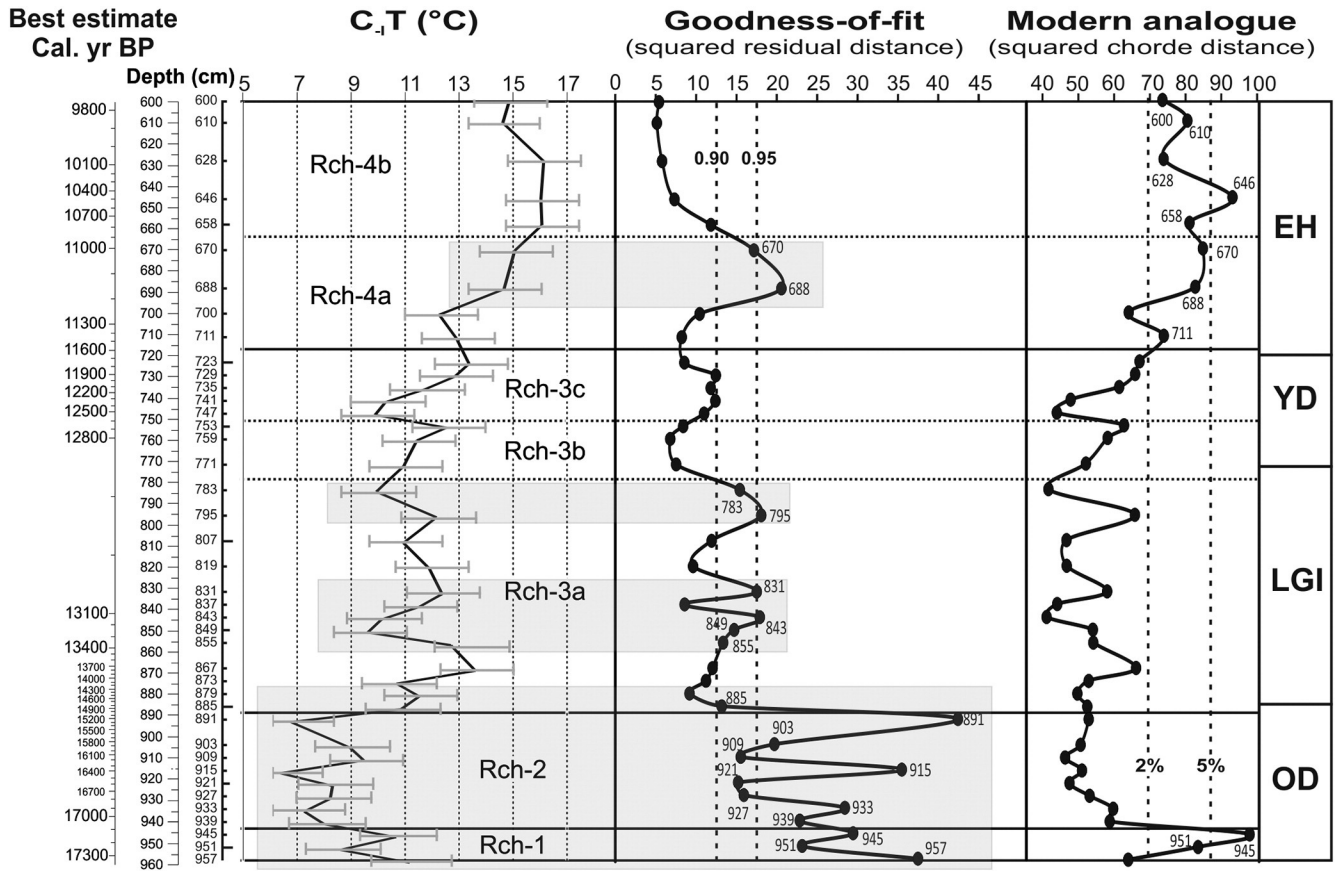

Fig. 5. From left to right, chironomid-inferred temperature estimates (C-IT) with sample specific error bars; goodness-of-fit of the fossil assemblages to temperature, vertical dotted line indicates the 90th and 95th percentiles of squared residual distances of modern samples to the first axis in a CCA, samples to the right of the line have a poor or very poor fit-to-temperature respectively; nearest modern analogue analysis, vertical dotted line indicates the 2nd and 5th percentiles of squared chord distances of the fossil sample to samples in the modern calibration dataset, samples to right of line have no close and no good modern analogue respectively. The shaded areas correspond to samples that should be considered as tentative and interpreted with caution. OD: Oldest Dryas; LGI: late-glacial interstadial; YD: Younger Dryas; EH: early Holocene.

Dryas seems to have been warmer with summer temperatures of about 13 °C, just before the early-Holocene climate improvement.

4.3. Diatom analysis

Sediment below 921 cm contained too few diatoms for counting. The core section analysed for diatoms, between 921 and 601 cm (Fig. 6), was partitioned into 10 diatom assemblages zones (RDaz1–10). The diatom flora of *Les Roustières* is composed of 149 species. For the statistical analyses, the original dataset was reduced to 65 samples and 132 species (species occurring in <2 samples at <0.2% were excluded). DCA axis 1 has a compositional turnover gradient length of 3.47 SD units and represents 20.9% of the variation in the diatom data. This gradient is most likely primarily related to the dissolved organic carbon (DOC) content, with minimal values during RDaz6 and a maximum in the upper part of the sequence in RDaz10. RDaz6 is dominated by small species of Fragilariaceae that are generally associated with low DOC while RDaz10 is dominated by *Aulacoseira* spp. that generally prefer humic waters with high DOC concentrations (Ginn et al., 2007). This general distribution can be observed in the few datasets developed in northern Europe (Stevenson et al., 1991) and northern America (Fallu and Pienitz, 1999; Enache and Prairie, 2002) in which DOC is found to represent a strong gradient. Although the actual values of the DOC optima and tolerance can be quite different between the datasets, as these depend on the range of the gradient, the *Aulacoseira* species appear to have consistently higher DOC optima than small-celled *Nitzschia* and Fragilariaceae species of the genera *Staurosirella*, *Staurosira*, and *Pseudostaurosira*. *Staurosira construens* var. *binodis* with a relatively high DOC optimum and a high score on DCA axis-1 represents one exception (Supplementary Table 1). Similarly in northern Sweden, Korsman and Birks (1996) find that *Aulacoseira* species (e.g. *A. ambigua*, *A. valida*, *A. nygaardii*) are more abundant in highly coloured lakes (i.e. with high DOC content) than in clear-water lakes in which small Fragilariaceae such as *Staurosirella lapponica* and *Pseudostaurosira pseudoconstruens* are more abundant. In the Austrian Alps, *Pseudostaurosira microstriata* and *Pseudostaurosira pseudoconstruens* are found to characterize very low DOC lakes, with their optima around 0.5 mg L^{-1} (Schmidt et al., 2004). In addition to DOC, DCA axis-1 may also represent a pH gradient as several acidophilous *Eunotia* spp. have a high DCA axis-1 score. The two variables DOC and pH, have been found to co-vary as the weak acids in DOC contribute to lowering the pH (Kingston and Birks, 1990,) although there is a complex relationship as chromophoric DOC can be degraded in strongly acidic lakes (Ginn et al., 2007). This explains why pH and DOC have also been found to be unrelated in various datasets (Dixit et al., 1993; Korsman and Birks, 1996). Nevertheless, changes in lake-water DOC are known to influence diatom distributions strongly as they affect water transparency, the underwater availability of light for photosynthesis via attenuation of photosynthetically active radiation, the thermal and mixing regimes of the surface layer, and chemical interactions controlling the bioavailability of nutrients and trace metals (Cameron et al., 1999; Fallu et al., 2002).

4.3.1. Zone RDaz1: samples 921 to 901 cm (ca 16,580 to15,765 cal yr BP, best estimate)

Assemblages in RDaz1 are relatively rich with $E(S_{300})$ up to 48 and are dominated by small Fragilariaceae such as *Staurosira venter*,

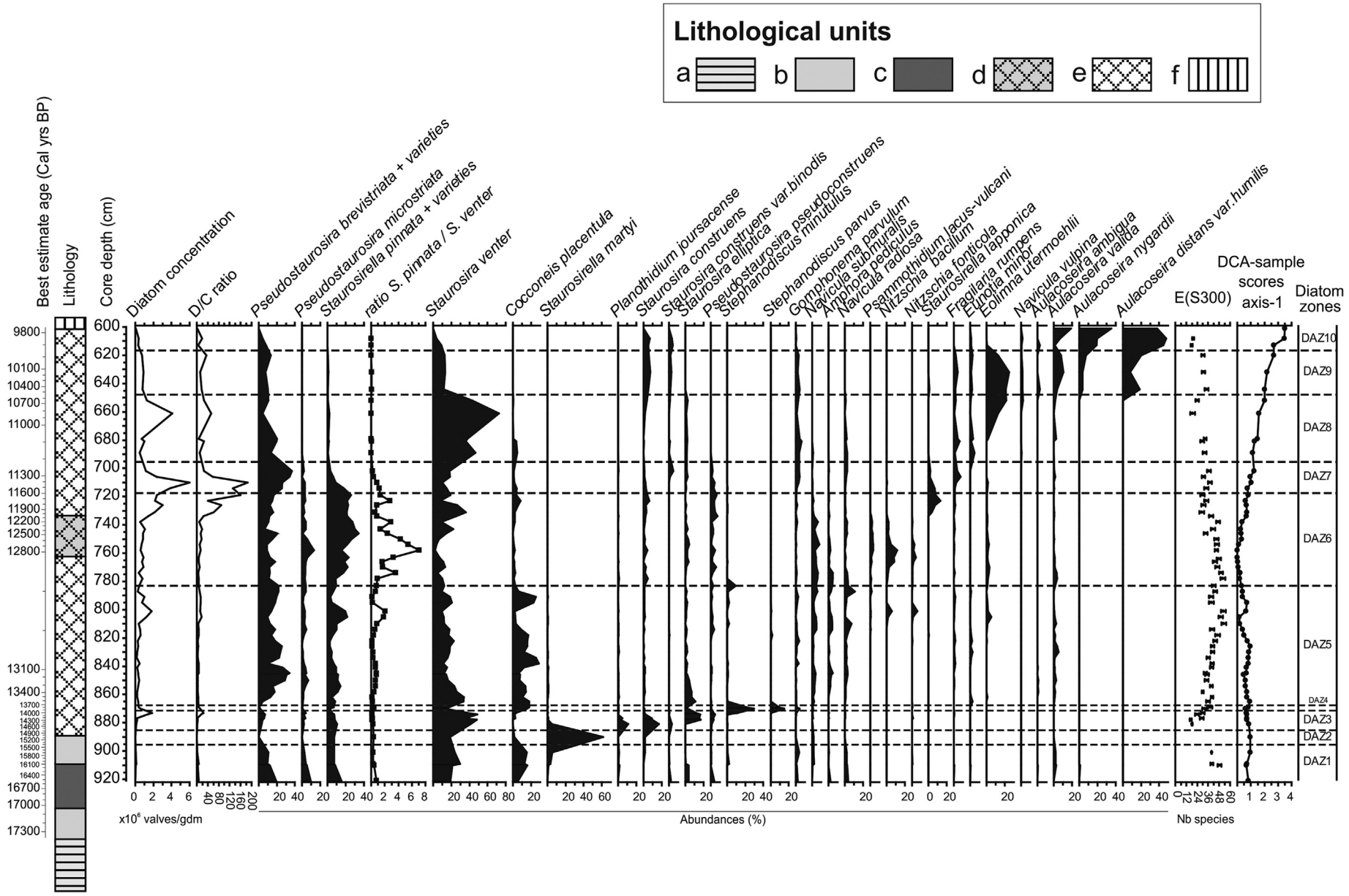

Fig. 6. Summary diagram showing selected diatom taxa encountered in *Les Roustières* sediments. The diagram zonation was determined using optimal sum of square partitioning (Birks and Gordon, 1985) using the software ZONE (Lotter and Juggins, 1991). The number of significant zones was determined by the "broken-stick" model using the BSTICK software (Birks and Line, unpublished). The names of lithological units (a–f) are given in Fig. 3.

Pseudostaurosira brevistriata, *Pseudostaurosira microstriata*, and *Staurosirella pinnata* and its varieties. The average diatom concentration in this zone is fairly low ($<1 \times 10^6$ valves mg^{-1}). Chrysophyte cysts are abundant and the D/C ratio varies from 2.4 to 6.5. Small Fragilariaceae are typically very abundant in pioneer diatom communities that dominate ponds and lakes in arctic (Laing and Smol, 2000; Finkelstein and Gajewski, 2008) and alpine regions (Lotter and Bigler, 2000) with extensive ice-cover. It is also interesting to note that in sediments formed at the time of deglaciation, fossil assemblages dominated by small Fragilariaceae are commonly reported in sediments deposited just after the retreat of the ice (Haworth, 1976). The small Fragilariaceae are primarily epipelic forms (Hickman, 1975). However, the epiphytic species *Cocconeis placentula* is also abundant (8 to 18%) in RDaz1 and suggests that aquatic macrophytes or mosses may have already been present in the lake.

4.3.2. Zone RDaz2: sample 890 (15,150 cal yr BP, best estimate)

This zone includes only one sub-sterile sample. Despite this, we decided to maintain this zone as its assemblage is clearly different from those in the samples above and below. Richness is very low (10 species). This is the only sample in which chrysophyte cysts are more abundant than diatoms (D/C ratio = 0.3). *Staurosirella martyi* is largely dominant (60%) in this sample. *Staurosirella pinnata* and *Staurosira venter* are subdominant species. *S. martyi* (=*Martyana martyi* = *Fragilaria leptostauron* var. *martyi*) has been reported as epipsammic, i.e. living on sand grains (Round et al., 1990). Mass occurrences of *S. martyi* have been often reported in calcium-rich sediments and in calcareous gyttja (Witkowski et al., 1995). This zone may therefore correspond to an episode of increased mineral influx to the lake, presumably as a result of erosion of less stable soils.

4.3.3. Zone RDaz3: samples 881 to 873 cm (14,560 to 14,050 cal yr BP, best estimate)

Compared with the previous zone, the average diatom concentration increases markedly to 0.7×10^6 valves mg^{-1}. The D/C ratio increases sharply up to 23. Assemblages are still dominated by small Fragilariaceae but become more diverse than in RDaz2 with *Staurosira venter*, *S. elliptica*, *S. construens*, *S. construens* var. *binodis*, *Pseudostaurosira pseudoconstruens*, *P. brevistriata*, *P. microstriata*, and *Staurosirella pinnata* and its varieties. *Planothidium joursacence*, generally described in the literature as a Nordic alpine species, is abundant (11%). $E(S_{300})$ increases through the zone, up to 30. The diatoms of this zone still indicate a pioneer assemblage.

4.3.4. Zone RDaz4: samples 870 to 869 cm (13,885 to 13,835 cal yr BP, best estimate)

This zone is characterized by a high abundance of the planktonic species *Stephanodiscus minutulus* (30%) and *S. parvus* (15%) combined with a sharp decrease in small Fragilariaceae and an increase of epiphytic diatoms such as *Cocconeis placentula* and *Gomphonema parvulum*. Diatom concentration declines slightly (0.4×10^6 valves mg^{-1}). Richness increases further, with $E(S_{300})$ up to 38. The two small planktonic *Stephanodiscus* species are typically associated with meso- to eutrophic conditions (Padisàk et al., 2009; Berthon et al., 2013). This zone suggests a deeper and more productive lake in which a truly planktonic diatom community could develop along with macrophytes. This suggests a large increase in the duration of the growing season.

4.3.5. Zone RDaz5: samples 865 to 788 cm (13,645 to 13,060 cal yr BP, best estimate)

Stephanodiscus species sharply decline and small Fragilariaceae again dominate the assemblages with *Pseudostaurosira brevistriata* and *Staurosira venter* as the most abundant species. *Aulacoseira valida* is common in the assemblages. Diatom concentration, on average, increases slightly. Richness increases markedly, especially towards the top of the zone with a peak value for $E(S_{300})$ of 53. This zone suggests a decrease in water depth such that planktonic diatoms could not develop large populations.

4.3.6. Zone RDaz6: samples 778 to 719 cm (13,015 to 11,640 cal yr BP, best estimate)

Percentages of small Fragilariaceae increase further with, in particular, high abundances of *Staurosirella pinnata*, *P. microstriata,* and *P. pseudoconstruens. Staurosirella lapponica* is only abundant at the top of the zone. *Staurosira venter* decreases markedly in the middle of the zone. Diatom concentration and the D/C ratio both increase sharply towards the top of the zone. The epipelic *Nitzschia bacillum* and *N. fonticola* are common. These small-celled *Nitzschia* are particularly good indicators of low DOC concentrations (Fallu and Pienitz, 1999; Fallu et al., 2002). Percentages of *C. placentula* decrease sharply, indicating a much reduced presence of macrophytes. Diatom richness declines throughout the zone, down to $E(S_{300})$ at 30. Interestingly, Birks et al. (2012) report from northern Norway during the same time interval a diatom assemblage totally dominated by *S. pinnata* that they interpret as indicating very cold and turbid waters. Studies on the modern distribution of these taxa in the Canadian Arctic (Joynt and Wolfe, 2001; Bouchard et al., 2004) and northern Sweden (Rosén et al., 2000) show that the various species of Fragilariaceae have different optima for summer water temperature with *Staurosirella* taxa living in colder water than *Staurosira* taxa. In circumpolar lakes in northern Russia, Laing and Smol (2000) find *Staurosirella pinnata* to be more abundant in the tundra zone, while *Staurosira venter* has higher abundances in lakes located at lower latitude in the boreal forest zone, and characterized by warmer surface water temperatures. Similar shifts in dominance between species of small Fragilariaceae have been observed in Canadian sequences, in which Podritske and Gajewski (2007) observed a clear inverse relationship between *Staurosira* and *Staurosirella.* Similarly, Finkelstein and Gajewski (2008) used the ratio of *Staurosirella pinnata* to *Staurosira venter* as an indicator for warm and cold phases in their record from the Canadian Arctic. The same ratio applied to *Les Roustières* diatom sequence clearly distinguishes RDaz6 as the coldest phase in our record. In support of this interpretation, *P. microstriata* has the lowest optima for July temperature and the highest optima for the length of ice-cover in a modern dataset from the Austrian Alps (Schmidt et al., 2004).

4.3.7. Zone RDaz7: samples 714 to 702 cm (11,510 to 11,240 cal yr BP, best estimate)

Assemblages are still dominated by small Fragilariaceae, although the percentages of the main species are different from those in the previous zone with lower *Staurosirella pinnata* and much higher *P. brevistriata.* Diatom concentration reaches its highest value for the whole profile (6×10^6 valves mg^{-1}) and chrysophyte cysts are very few. Richness remains at a relatively low level with $E(S_{300})$ between 31 and 38. Epiphytic species such as *Gomphonema parvulum* and *Fragilaria rumpens* are common. The sharp decline in the *S. pinnata*/*S. venter* ratio and the apparent increase in aquatic vegetation and in productivity suggest warmer conditions than in the previous zone.

4.3.8. Zone RDaz8: samples 689 to 652 cm (11,100 to 10,660 cal yr BP, best estimate)

Staurosira venter largely dominates the assemblage while *P. brevistriata* decreases. Towards the top of the zone motile, epipelic species such as *Eolimna utermoehlii* and the large-celled *Navicula vulpina* increase markedly while epiphytic species decrease. Diatom concentration decreases while chrysophyte cysts become more abundant. Diatom richness declines markedly towards the top of the zone with $E(S_{300})$ down to 18. The increase in the relative abundance of *Eunotia minor,* a species regularly found on mosses (Alles et al., 1991; Bertrand et al., 2004; Pavlov and Levkov, 2013) may indicate the development of a peat bog.

4.3.9. Zone RDaz9: samples 644 to 620 cm (10,450 to 9925 cal yr BP, best estimate)

Assemblages are dominated by the planktonic *Aulacoseira valida*, *A. nygaardii*, and *A. distans* var. *humilis* while the abundance of *Eolimna utermoehlii* (=*Navicula subrotundata*) increases further. Diatom concentration decreases further (0.8×10^6 valves mg^{-1}) and richness increases with $E(S_{300})$ above 30. The *Aulacoseira* spp. indicate fairly high concentrations of DOC (Supplementary Table 1; Stevenson et al., 1991; Fallu and Pienitz, 1999; Enache and Prairie, 2002). Low levels of light, generally associated with high DOC, may have been favourable to large populations of *E. utermoehlii* that was reported as a characteristic benthic motile diatom of deep-water assemblages (Kingston et al., 1983). This species is also found to be associated with warm and nitrogen-rich waters (Kocev et al., 2010).

4.3.10. Zone RDaz10: samples 613 to 601 cm (9845 to 9785 cal yr BP, best estimate)

In this zone the diatom concentration decreases significantly from 0.3 to 0.06 × 106 valves mg^{-1}. Samples above 601 cm are sterile. The assemblages are characterized by dominant *Aulacoseira distans* var. *humilis* and by subdominant *A. nygaardii* (60–70% together). The last sample is almost entirely composed of cingulum of *Aulacoseira* spp. with no entire valves. Diatom richness decreases with $E(S_{300})$ below 20. *Eolimna utermoehlii* declines sharply and epiphytic diatoms almost disappear from the assemblages, which suggest the decline of macrophytes and may relate to low light conditions unfavourable for benthic diatoms. The relative dominance of planktonic *Aulacoseira* spp. and low diatom concentration suggest dystrophic conditions, characterized by low phytoplankton production and high organic content (Wetzel, 2001).

5. Discussion

5.1. Past lacustrine environmental reconstruction based on multiproxy evidence (comparison between diatom, chironomid, pollen, and lithological results)

5.1.1. Oldest Dryas period (RCh1–2, RDaz1–2, grey clayey sediment)

The base of the sequence at *Les Roustières*, between 17,700 to 16,600 cal yr BP is marked by the absence of diatoms, whereas chironomids are well represented. This may be due to high water turbidity or persistent ice-cover (due to extreme climate conditions), which may have decreased the amount of light available for photosynthetic activities, and thus strongly reduced lacustrine primary productivity. Alternatively, relatively high pH and a low silica concentration may have caused poor preservation of diatom remains. The contemporaneous chironomid assemblages are composed mainly of profundal, cold, oligotrophic taxa. This is also supported by the sedimentation of clay. Summer temperatures during this period were lower than or equal to 10 °C (Fig. 7) which is not favourable for high lacustrine productivity. The sub-sterile RDaz2 zone is also contemporaneous with a minimal summer temperature of around 7 °C. At the end of the Oldest Dryas, between ca 16,400 and 15,000 cal yr BP, chironomids and diatoms together point to a cold oligotrophic (to mesotrophic) lake with shallow waters, with the probable presence of aquatic macrophytes on littoral margins. However, very few pollen grains of *Potamogeton* and *Myriophyllum* were recorded in the pollen analysis (Fig. 3).

5.1.2. Late-glacial interstadial (RCh3a, RDaz3–5 and gyttja sediment)

Both diatom and chironomid evidence suggest that the onset of the late-glacial interstadial (LGI) is marked by taxonomic diversification,

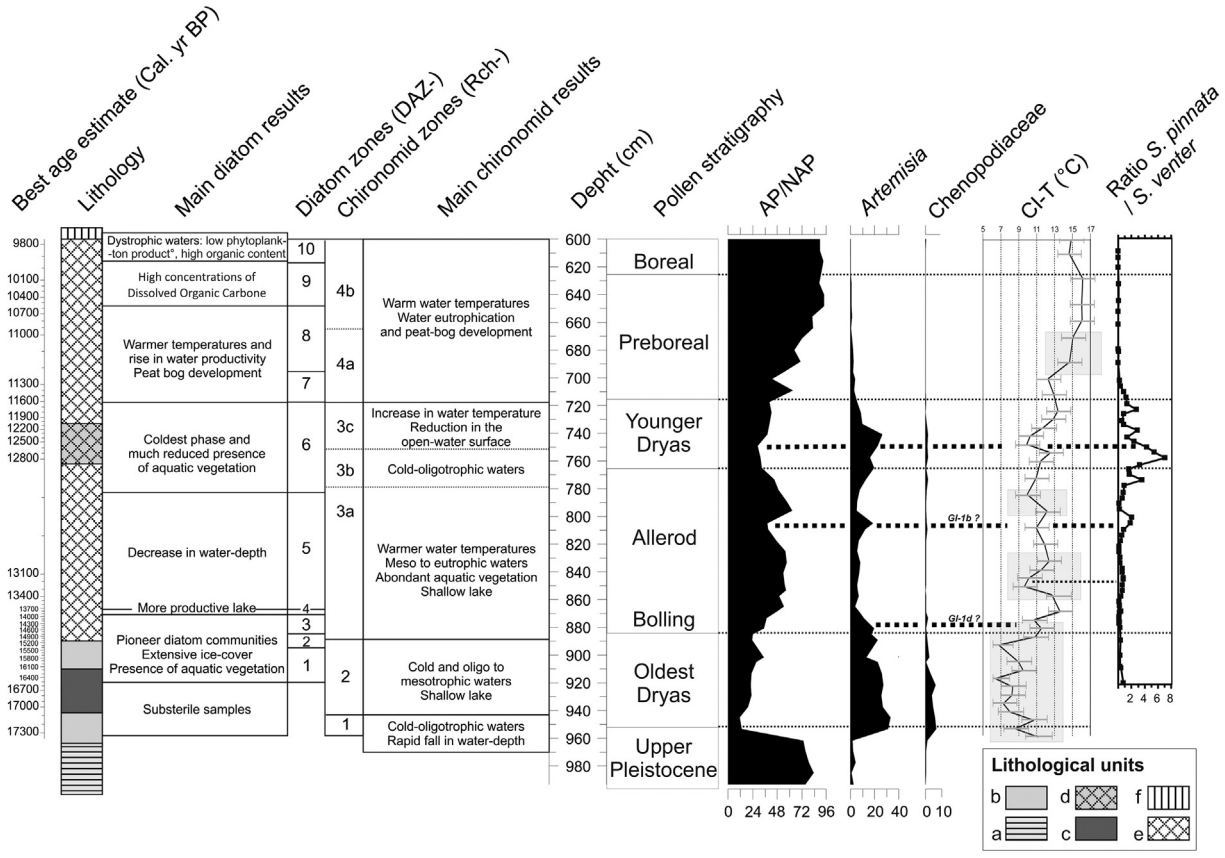

Fig. 7. Comparison between the pollen stratigraphy, lithology, chironomid-inferred temperature reconstruction (CI-T), and the diatom ratio *Staurosirella pinnata*/*Staurosira venter*. The names of lithological units (a–f) are given in Fig. 3.

moderate water eutrophication, and growth in aquatic vegetation, probably in response to climatic improvement. This is confirmed by an increase in *Potamogeton* and *Myriophyllum* abundance (Fig. 3). However, the abundances of both cold-adapted diatoms and chironomids over the LGI seem to indicate relatively moderate but unstable summer temperatures (never exceeding 14 °C), as shown by the fluctuating chironomid-inferred temperature curve and the *S. pinnata*/*S. venter* ratio (Fig. 7). A probable cold event is indicated by pollen data from *Les Roustières* that show a sharp decrease in the AP/NAP ratio around 13,000 cal yr BP (Fig. 7), related to rises in *Artemisia* and Poaceae percentages. This vegetation dynamic is contemporaneous with a slight rise in the *S. pinnata*/*S. venter* ratio only. This cold event, may be related to the GI-1b cold event recorded in the NGRIP ice-core, which is also named the Intra-Allerød Cold Period in terrestrial records from the North Atlantic region or the Gerzensee oscillation in central European lakes.

5.1.3. Younger Dryas (RCh3b-c, RDaz6 and clay-gyttja sediment)

The Younger Dryas event is well marked in both the diatom and chironomid assemblages, as shown by the decrease or absence of thermophilous chironomid taxa and the simultaneous rise in the *S. pinnata*/*S. venter* ratio. This climatic deterioration is also indicated in the pollen results with a fall in the AP/NAP ratio that is associated with decreasing percentages of *Pinus* and increasing percentages of the steppic taxa *Artemisia* and Chenopodiaceae (Fig. 3).

In addition, the YD event induced a change in the hydrological regime of the basin with more oligotrophic water and a probable decrease in the input of allochthonous organic matter (as suggested by the increase in abundances of the diatoms *Nitzschia fonticola* and *N. bacillum* that indicate low DOC concentrations). This may have been a consequence of the freezing of small rivulets feeding the lake during the major part of the year. Lastly, a decrease in macrophytes is indicated by the fall in macrophyte associated diatoms (e.g. *Cocconeis placentula*) and chironomids such as *Dicrotendipes* in RCh-3b sub-zone, which is consistent with slightly lower abundances of *Potamogeton* and *Myriophyllum* (Fig. 3) than during the LGI.

5.1.4. Early Holocene (RCh4, RDaz7–10, organic gyttja and peat)

Both macrophytic chironomid fauna (such as *Glyptotendipes*, *Dicrotendipes* and *Polypedilum*) and epiphytic diatom species (such as *Gomphonema parvulum* and *Fragilaria rumpens*) show a shallowing of the lake with climatic improvement that occurred at the beginning of the Holocene. Maximal abundances of *Potamogeton* and *Myriophyllum* (Fig. 3) indicate dense hydrophytic vegetation into the persistent open waters close to the extended peat-bog. Palustrine environment is also indicated by the increasing abundances of the acidophilic chironomid taxa such as *Ablabesmyia* cf. *phatta* and *Psectrocladius sordidellus* (Fig. 4) and diatoms such as *Aulacoseira* spp. (Fig. 6). *Les Roustières* basin was probably largely filled-in at that time.

5.2. Reliability of the chironomid-based temperature reconstruction

Several samples, especially those in the Older Dryas, have a poor-fit-to-temperature. Moreover, DCA sample scores (Fig. 4) show that while the axis 2 scores reflect the major trends in the C-IT reconstruction, the axis 1 scores, which reflect the major environmental driver of the chironomid assemblage composition, show a different pattern. These results suggest that variables other than temperature may have been influencing the response of the chironomid assemblages at this time. Other variables known to influence chironomid distribution and abundance include water depth, pH oxygen conditions, and trophic level (Brooks et al., 2016; Juggins, 2013). Hence, this raises the question about the major forcing factor for the chironomid fauna at *Les Roustières*. The chironomid fauna is dominated from the Older Dryas to the end of the Younger Dryas by *C. ambigua,* which has a strong influence on the temperature reconstruction, as indicated by the striking inverse correlation between *C. ambigua* percentage abundance, the temperature curve and the DCA axis 1 scores. *C. ambigua* has an ambiguous response to temperature (Brodersen and Lindegaard, 1999) and it may also be responding to the natural infilling of the site and fluctuations in lake-level. However, it is clear that the CI-T is correlated with the main floristic and diatom changes. The temperature (CI-T) decreases are contemporaneous with both landscape openings and rise in the *S. pinnata* / *S. venter* ratio, which argues for cold climate conditions (Fig. 7). These evidences makes us confident that temperatures were relatively low during the Older Dryas part of the sequence.

5.3. Regional comparison

The first attempt at a climate reconstruction at the Taphanel site was done by Ponel and Coope (1990), based on fossil Coleoptera assemblages using the Mutual Climatic Range method (Atkinson et al., 1987). The Taphanel record is located within 80–100 km of *Les Roustières* peat bog and at an elevation of almost 1000 m asl. With the exception of the difference in elevation between the two sites, the two records are located in a similar climate context that allows direct comparison (Table 2) between chironomid-inferred July temperature and T_{MAX} (mean temperature of the warmest month). The chironomid-inferred temperature reconstruction has a better sampling resolution and a lower temperature range but is in good agreement with the MCR data, especially when temperature ranges for coleopteran data are narrow.

According to Ponel and Coope (1990), the late Würm and Oldest Dryas climates were of arctic severity and considerably more continental than at present. MCR coleopteran reconstructions have shown that summer temperatures ranged from 7 to 13 °C. Chironomid data suggest that the mean July air temperatures ranged probably from 6 to 10 °C.

The Ponel and Coope (1990) reconstructions show a climatic warming at about 13,000 uncalibrated yr BP (about 15,000 cal yr BP) followed by the Bølling temperate episode. This climate improvement is confirmed by the rise in chironomid-inferred temperatures just after 15,200 cal yr BP (cf., best estimate age). However, based on chironomid data, this warming is moderate compared to the maximum values suggested by MCR. This cooler climate is confirmed by the abundance of cold diatom species at *Les Roustières* throughout the LGI.

Ponel and Coope (1990) identified a marked deterioration in summer warmth for a short period between the Bølling and Allerød, which is perhaps the Older Dryas period. Nevertheless, we note that this interpretation is not supported by an increase in cold beetle species but only by the MCR inference being better constrained for this particular sample. In addition, the absence of both absolute ^{14}C dating and an age-depth model for La Taphanel record and the low sample resolution of the coleopteran analysis, make it impossible to establish a more accurate chronological correlation with *Les Roustières* for this interval.

As suggested by the Coleoptera at La Taphanel, the Allerød period was decidedly cooler than the Bølling. The chironomid data from *Les Roustières* do not confirm this hypothesis, with maximum temperatures reached between 13,800 and 13,400 cal yr BP, during the Allerød. Nevertheless, midges suggest that the Allerød period was marked by climate instability (confirmed by several proxies cf., Fig. 7) occurring between 13,300 and 12,900 cal yr BP. It is also possible that the Coleoptera analysis failed to detect such a short-lasting event due to its coarse temporal resolution, as the large volume of sediment required for this type of analysis results in very thick samples of low temporal resolution. This may lead to the pooling of cool and warm phases and thus to an under- or over-estimation of the coleopteran T_{MAX} values.

At La Taphanel, the climate deterioration of the Younger Dryas is marked by a drop in summer temperatures with a probable return to conditions similar to the Oldest Dryas and a rise in continentality. The chironomid record from *Les Roustières* suggests that this cooling in summer temperatures was somewhat limited, as Younger Dryas Tjul were 2–3 °C higher than those of the Oldest Dryas. This has already been

Table 2
Temperature comparisons between late-glacial European records. Numbers in brackets indicate temperature ranges ("+" warming; "−" cooling). *Corrected values have been calculated with elevational and latitudinal correcting factors, using the lapse rates of 0.6 °C per 100 m elevation and 0.6 °C per 1° latitude, which are often used for summer temperatures. These corrected values correspond to probable values that the reference site would have received if it was located at the same latitude and elevation as Les Roustières.

Location	References	Oldest Dryas	Corrected values*		Bølling	Corrected values*		Allerød	Corrected values*		Younger Dryas	Corrected values*		Early Holocene	Corrected values*	
Les Roustières (1196 m)	This study	6 to 10 °C	–	–	11 °C (+4 °C)	–	–	12 to 13 °C (+1 to 2 °C)	–	–	ca 10° & 13 °C (−2 °C)	–	–	12 to 16 °C (+3 °C)	–	–
Lautrey (788 m)	Peyron et al. (2005)	11 to 12 °C	10.3	11.3	15.5 to 16 °C (+5 °C)	14.8	15.3	15.5 to 18.4 °C (+2 to 3 °C)	14.8	17.7	13.6 to 13.9 °C (−3 to −4 °C; sec. part +0.3 °C)	12.9	13.2	13.9 to 15.5 °C (+1.5 to 3 °C)	13.2	14.8
Lautrey (788 m)	Heiri and Millet (2005)	11 to 12 °C	10.3	11.3	14 to 16 °C (+3 to 3.5 °C)	13.3	15.3		15.8	16.7	14 to 15 °C (−2.5 to −3.5 °C)	13.3	14.3	16°5	15.8	–
Ech (710 m)	Millet et al. (2012)	10 to 13 °C	6.7	9.7	16 to 17.5 °C (+6 °C)	12.7	14.2	ca. 16.5 °C (−1 °C) 16.5–17 °C	13.2	–	15 to 15.5 °C (−1.5 °C)	11.7	12.2	ca. 17 °C	15.7	–
La Taphanel (975 m)	Ponel and Coope (1990)	7 to 13 °C	6.0	12.0	11 to 23 °C	10.0	22.0	11 to16°C	10.0	15.0	6 to 18 °C	5.0	17.0	10 to 23 °C	9.0	22.0
Gerzensee (603 m)	Lotter et al. (2012)	About 11 °C	9.3	–	12 to 14 °C (+2 to 3 °C)	10.3	12.3	14 to 16 ° C	12.3	14.3	–	–	–	–	–	–
Egelsee (770 m)	Larocque-Tobler et al. (2010)	ca. 11.4 °C	11	–	ca. 17 °C (+3 to 4 °C)	16.6		ca. 15.5 °C	15.1	–	ca. 13.9 °C (−1.5 °C)	13.5		Average of 15.3 °C (+3 °C)	14.9	–
Hinterburgsee (1515 m)	Heiri et al. (2003)	–	–	–	–	–	–	–	–	–	10.4 to 10.9 °C	14.2	14.7	11.9 to 12.8 °C	15.7	16.6
Maloja pass (1815 m)	Ilyashuk et al. (2009)	–	–	–	–	–	–	10 to 11.7 °C	15.6	17.3	8.8 & 9.8 °C (−3.5 to −4 °C)	14.4	15.4	13.6 to 13.9 °C (−3.5 to −4 °C)	19.2	19.5
Lago di Piccolo (365 m)	Larocque and Finsinger (2008)	ca.16 °C (only one sample)	14.3		ca. 19 °C (+3 °C)	17.3		ca. 17 °C	15.3	–	ca. 16 °C (−1.5 °C)	14.3		ca. 18.5 °C (+2.5 °C)	16.8	
L. di Lavarone (1(100 m)	Heiri et al. (2007b)	10.5 to 10.8 °C	11.2	11.5	13.8 to 13.9 °C (+3 °C)	14.5	14.6	15.3 °C just before YD	16.0	–	11.7 to 14.5 °C (−2 °C)	12.4	15.2	15.8 to 16.4 °C (+2.5 °C)	16.5	17.1
Hijkermeer (14 m)	Heiri et al. (2007a)	–	–	–	14 to 16 °C imprecise ^{14}C	12.4	14.4	16 to 16.5 °C	14.4	14.9	13.5 to 14 °C (−2 to −3 °C)	11.9	12.4	15.5 to 16 °C (+2 to 3 °C)	13.9	14.4
Five sites (8 to 250 m)	Lang et al. (2010)	–	–	–	12 to 13 °C	12.5	13.5	–	–	–	8 to 10 °C (average of −4.5 °C)	8.5	10.5	15.5 to 16 °C (+5 °C)	16.0	16.5
Haweswater (8 m)	Bedford et al. (2004)	7.4 to 10 °C	6.5	9.1	ca.13.4 °C (+3 to +4 °C)	12.5	–	ca. 11.4 °C (−2 °C)	10.5	–	7.5 °C & 10 °C (− 6 °C)	6.6	9.1	13.8 °C (+4 to 5 °C)	12.9	–
L. Nadourcan (70 m)	Watson et al. (2010)	7.5° to 9 °C	7.6	9.1	ca. 13 °C (+5 °C)	13.1	–	ca. 12 °C (−1 to −2 °C)	12.1	–	7.5 to 10 °C (−5 °C and +2.5 °C over the YD)	7.6	10.1	Around 14 °C (+4 to 5 °C)	14.1	–
Whitrig Bog (125 m)	Brooks and Birks (2001)	6 °C (only one sample)	–	6.8	10.5 to 12 °C (+5 to 6 °C)	11.3	12.8	ca.11 °C (−1° over the YD)	11.8	–	7.5 °C to 9 °C (−2.5 to −3.5 °C)	8.3	9.8	11.5 °C (+2.5 °C)	12.3	–

Location	References	GI-1d	Corrected values*		GI-1b	Corrected values*		PBO	Corrected values*	
Les Roustières	This study	10 °C (−1 °C)	–		– (−1 °C)	–	–	– (−0.5 to −1 °C)	–	–
Lautrey (788 m)	Peyron et al. (2005)	ca. 15 °C (−0.75 to −1 °C)	14.3		16.8 to 15 ° C (−2 °C)	14.3	16.1	17.5 to 14 °C (−3.5 °C)	13.3	16.8
Lautrey (788 m)	Heiri and Millet (2005)	–	–		– (−1.5 to −2 °C)	–	–	–	–	–
Ech (710 m)	Millet et al. (2012)	– (−1.5 °C)	–		–	–	–	–	–	–
La Taphanel (975 m)	Ponel and Coope (1990)	–	–		–	–	–	–	–	–
Gerzensee (603 m)	Lotter et al. (2012)	– (−0.5 to −1 °C)	–		–	–	–	–	–	–
Egelsee (770 m)	Larocque-Tobler et al. (2010)	–	–		–	–	–	− (−1 °C)	–	–
Hinterburgsee (1515 m)	Heiri et al. (2003)		–			–	–	10.4 to 11.1 °C (−0.8 °C)	14.1	14.9
Maloja pass (1815 m)	Ilyashuk et al. (2009)	ca 9 °C (−2.1 °C)	14.6		ca 6 °C (−1.4 °C)	11.6	–	–	–	–
Lago di Piccolo (365 m)	Larocque and Finsinger (2008)	–	–		–	–	–	–	–	–
L. di Lavarone (1(100 m)	Heiri et al. (2007b)	–	–		–	–	–	− (−0.5 °C)	–	–
Hijkermeer (14 m)	Heiri et al. (2007a)	– (−1.5 °C)	–		– (−2.1 °C)	–	–	–	–	–
Five sites (8 to 250 m)	Lang et al. (2010)	– (−0.6 to −2.6 °C)	–		– (−0.8 to −1.6 °C)	–	–	− (up to −1 °C)	–	–
Haweswater (8 m)	Bedford et al. (2004)	No date; (−1 to −1.5 °C)	–		–	–	–	− (−1 to −1.5 °C)	–	–
L. Nadourcan (70 m)	Watson et al. (2010)	ca.11 °C (−2.5 °C)	11.1		ca. 12 °C (−1 to −1.5 °C)	12.1	–	–	–	–
Whitrig Bog (125 m)	Brooks and Birks (2001)	ca. 8 °C (−1.5 to −2 °C)	8.8		About 9.5 °C (inferior to −1 °C)	10.3	–	–	–	–

shown by Heiri et al. (2014) for CI-T records from southern Europe (and central Europe) where the early late-glacial (ELG)was cooler than the Younger Dryas; a situation that can be explained by the more southerly position of North Atlantic sea-ice during the ELG (Renssen and Vandenberghe, 2003). At *Les Roustières*, the early-Holocene climatic improvement as recorded by the chironomid-inferred temperature shows a good correlation with the coleopteran MCR inferences from La Taphanel, and reduces the previous range of coleopteran MCR of 10–20 °C to a CIT range of 12–16 °C.

5.4. Comparison with other European palaeoecological data

5.4.1. Oldest Dryas–Bølling climate transition

The chronology of this major climate transition is poorly documented in most of the published palaeoecological records and comparison with chironomid data from *Les Roustières* must therefore be carefully addressed. This chronological problem has recently been discussed by Moreno et al. (2014) who compared trends of climate change across the interglacial on a north-south transect in Europe. Nevertheless, European chironomid-inferred temperature records, from sites such as Lake Lautrey (Heiri and Millet, 2005), Lake Ech (Millet et al., 2012), Egelsee (Larocque-Tobler et al., 2010), Lago di Lavarone (Heiri et al., 2007b) and Lough Nadourcan (Watson et al., 2010) are relatively well chronologically documented, which allows a comparison between them and the summer temperature record from *Les Roustières*. In the discussion below the chironomid-inferred temperatures from other sites were re-calculated to the elevation of *Les Roustières* using both altitudinal and latitudinal lapse rates of 0.6 °C/100 m and 0.6 °C/1° of lat., respectively (see Table 2 for details).

The Oldest Dryas Tjul from *Les Roustières* is close to or slightly cooler than, the summer temperatures inferred from pollen and chironomids from Lake Lautrey in the Jura (Heiri and Millet, 2005; Peyron et al., 2005), and from Lake Ech in French Pyrenees (Millet et al., 2012). Hence, the cooler temperatures inferred for *Les Roustières* probably reflect the elevational difference as *Les Roustières* is about 400 m higher than the Jura site, and by the more southerly location of the Pyrenees site. In the Massif Central and Jura sites, the rapid climate warming that occurred at the onset of the Bølling (cf. Greenland Interstadial 1: GI-1) at around 15,000 cal yr BP, is approximately of the same amplitude. As suggested by Peyron et al. (2005), this warming of 4–5 °C is consistent with other palaeoecological results from western and central Europe (see Peyron et al., 2005 for a summary of these data). This is also similar to the amplitude of warming of 3–6 °C reconstructed from chironomids in many European records (Table 2). This change was rapid and occurred over approximately 300 years (i.e. an increase of about 1.3–1.6 °C per century). Recently, Moreno et al. (2014) highlighted that the onset of GI-1 was more abrupt in northern records than in southern ones and that this difference cannot be solely related to differences in the accuracy of the age models.

5.4.2. Late-glacial interstadial (LGI): Bølling-Allerød period

One of the recurrent questions discussed during the last three decades concerns the temperature differences between the onset and the termination of the LGI. Many studies based on coleopteran analysis from northern Europe (e.g. Britain and southern Sweden) have reconstructed Bølling summer temperatures to be warmer than those for the Allerød (Coope and Lemdahl, 1995). This differs from the interpretation of pollen data, based on the relative increase of the arboreal pollen against non-arboreal pollen through the LGI, which might suggest that the Allerød was warmer than the Bølling. According to Hoek (2008), however, these data show that the warmest phase occurred during the Bølling, when the extent of the trees was limited. Hoek (2008) formulated this hypothesis based on British and Swedish records and was confirmed by the Greenland ice-core records (GRIP and GISP2). Such gradual cooling throughout GI-1 is also apparent at several sites in NW England based on chironomid evidence (Bedford et al., 2004; Lang et al., 2010), Ireland (Watson et al., 2010), and Scotland (Brooks and Birks, 2001). Moreno et al. (2014) suggest there is a North–South European gradient through GI-1 in which GI-1a is warmer than GI-1e in the south but cooler in the north.

Ponel et al. (2005) show a different climate trend during the LGI for northern France, where there is little or no evidence for cooling during the Allerød interval. These results are similar to climatic reconstructions from Hauterive-Champréveyres, Switzerland, (Coope and Elias, 2000) and at Grand Marais (Gaillard and Lemdahl, 1994). Several chironomid-inferred temperature records from mid-European latitudes, such as Lago di Lavarone (Heiri et al., 2007b), Hijkermeer (Heiri et al., 2007a), Gerzensee (Lotter et al., 2012), and Lautrey (Heiri and Millet, 2005), show an increase in summer temperatures from the Bølling to the Allerød. At *Les Roustières* a warmer phase (+1.5 to 2 °C) may occur between 13,800 and 13,300 cal yr BP (during the Allerød). The only European CI-T records which show a climatic cooling trend in the interstadial are from Egelsee and Lago Piccolo di Avigliana (LPA). However, at LPA (Larocque and Finsinger, 2008) only one sample was analysed in the Bølling, while at Egelsee (Larocque-Tobler et al., 2010), only one sample in the Bølling rises to 18 °C. The others are less than the average Allerød temperatures. Hence, based on the European insect data, it appears that there were different climate trends between northern Europe and central Europe during the LGI. These thermal differences are probably due to variations in North Atlantic surface-water temperatures, as also suggested by Heiri et al. (2014). Renssen et al. (2009) find that before 7000 cal yr BP, summers were substantially cooler in regions directly influenced by the presence of the Laurentide ice-sheet, whereas in other regions in the Northern Hemisphere summer temperatures were dominated by orbital forcing. These authors argue that the cool conditions are related to the inhibition of the Labrador Sea deep convection by the flux of meltwater from the ice-sheet, which weakened northward heat transport by the ocean. This may have had a strong influence on the late-glacial and early-Holocene climate over NW Europe such as Iceland, Ireland, and NW England, but was less influential in central Europe where insolation is the main climate driver. Competing influences from variations in North Atlantic surface-water temperature, the proximity of the Fennoscandian ice-sheet, and seasonal variations over the ice-free continent are discussed by Coope et al. (1998) as possible causes of the thermal gradient across northern Europe at the late-glacial–Holocene transition and this point has been discussed further by Moreno et al. (2014).

5.4.3. The Younger Dryas stadial and early-Holocene climate warming

In records from south-western Europe (cf. Heiri et al., 2014; Millet et al., 2012; Muñoz Sobrino et al., 2013), the range in YD summer temperatures changes appears to be weaker than elsewhere in Europe (e.g. British Isles, Baltic region). This is probably due to latitudinal shifts and restructuring in the oceanic surface current circulation over the North Atlantic area. Indeed, the moderate CI-T change during YD at *Les Roustières* (−2 °C) is consistent with south-western CI-T records such as Ech (Millet et al., 2012), Lago di Piccolo (Larocque and Finsinger, 2008) and Lago di Lavarone (Heiri et al., 2007b), whereas northern records such as those studied by Lang et al. (2010) or Watson et al. (2010) have shown a drop in summer temperatures of about 4–6 °C (Table 2).

At *Les Roustières*, chironomid-inferred temperatures indicate a probable strong warming (+3 °C) in the second and terminal part of the Younger Dryas (between 12,200 and 11,700 cal yr BP), which is consistent with the bipartite climate division of the period detected both by Peyron et al. (2005) in Jura and Ilyashuk et al. (2009) in the Central Swiss Alps. Peyron et al. (2005) argue for a cold first part (around 11 °C) and a warmer second part (13–14 °C) in records from Switzerland, Germany, and central and north-western Europe.

Finally, at *Les Roustières*, according to the CI-T reconstruction, a second temperature increase of about 3 °C can be observed after

11,300 cal yr BP. This early-Holocene warming appears to be delayed with regard to the date of 11,653 cal yr BP proposed by the INTIMATE-group (Lowe et al., 2008). However, this temporal offset should not be overemphasized considering both the sample resolution of the *Les Roustières* sequence and the error margins in the age depth model. In any case, these thermal improvements are close to the values of a 2.5–3 °C warming recorded at the beginning of the Holocene at Lake Lautrey, in the Netherlands, and in Swiss and northern Italian Alps (Table 2) or in central Europe (Isarin and Bohncke, 1999). Again, the values for the British Isles are higher (e.g., Lang et al., 2010). Moreno et al. (2014) have shown that northern European records indicate a larger temperature increase at the onset of the Holocene than at the onset of GI-1. These authors hypothesise that alpine records and southern European reconstructions show similar temperature variations during these two major climate warming episodes. However they caution that more temperature reconstructions, especially from southern regions of western Europe are necessary to confirm this observation. The *Les Roustières* record serves to strengthen this hypothesis.

6. Conclusions

The quantitative reconstruction of past summer temperature at *Les Roustières* based on chironomid assemblages cross-correlated with diatom and pollen evidences, has shown that climatic events of the late-glacial termination, such as the LGI and early Holocene climate improvements and Younger Dryas cold events are recorded in *Les Roustières* sequence with probable magnitudes of about +4 °C, +3 °C, and −2 °C, respectively. The Massif Central climate trend, in regard to the ranges of temperature changes, seems similar to those recorded in central and south-western Europe but differs from those from sites in Britain and Ireland. This thermal offset was probably caused by differences in the relative influence of the North Atlantic Ocean on the climate of north-western Europe.

Finally, the record shows that the LGI climate in the Aubrac region was probably slightly colder than at lower elevations in France (Lake Lautrey and Lac Ech) or in Swiss and north Italian alpine lakes (Lago di Piccolo, Lago di Lavarone). These cool conditions are still prevalent today and are related to the geographical position of the Massif Central; located at a climatic crossroad between the oceanic westerlies and the contrasting cold continental and temperate Mediterranean air masses. This configuration is particularly favourable to temperature inversion and stagnation in winter. This cold climate context may explain the regional survival of a few glacial relict species (e.g., *Ligularia sibirica*, *Somatochlora arctica*, *Coenagrion lunulatum*, etc.)

Supplementary data to this article can be found online at http://dx.doi.org/10.1016/j.palaeo.2016.08.039.

Acknowledgements

This study was funded by the CNRS-Eclipse program. Radiocarbon analysis was done by JP. Dumoulin and C. Moreau at the "*Laboratoire de Mesure du Carbone 14*", CEA-ARTEMIS facility, Gif sur Yvette (France). Thanks are due to Céline Boursier and Gaëlle Lacroix for their help during laboratory works, respectively. We also thank the residents of Malbouzon (Aubrac, France) for their hospitality during the field campaign.

References

Alles, E., Nörpel-Schemp, M., Lange-Bertalot, H., 1991. Zur Systematik und Ökologie charakteristicher *Eunotia*-Arten (Bacillariophyceae) in elektrolytarmen Bachoberläufen. Nova Hedwigia 53 (1–2), 171–213.
Atkinson, T.C., Briffa, K.R., Coope, G.R., 1987. Seasonal temperatures in Britain during the past 22,000 years, reconstructed using beetle remains. Nature 325, 587–592.
Ayral, M., 1928. Le plateau d'Aubrac. Ann. Géogr. 37, 224–237.
Barley, E.M., Walker, I.R., Kurek, J., Cwynar, L.C., Mathewes, R.W., Gajewski, K., Finney, B.P., 2006. A northwest North American training set, distribution of freshwater midges in relation to air temperature and lake depth. J. Paleolimnol. 36, 295–314.
Battarbee, R.W., Kneen, M.J., 1982. The use of electronically counted microspheres in absolute diatom analysis. Limnol. Oceanogr. 27, 184–188.
Beaulieu, J.L., Pons, A., Reille, M., 1985. Recherches pollenanalytiques sur l'histoire Tardiglaciaire et Holocène de la végétation des monts d'Aubrac (Massif Central, France). Rev. Palaeobot. Palynol. 44, 37–80.
Bedford, A., Jones, R.T., Lang, B., Brooks, S., Marshall, J.D., 2004. A Late-glacial chironomid record from Hawes Water, Northwest England. J. Quat. Sci. 19, 281.
Bennett, K.D., 1996. Determination of the number of zones in a biostratigraphical sequence. New Phytol. 132, 155–170.
Berezina, N.A., 2001. Influence of ambient pH on freshwater invertebrates under experimental conditions. Russian Journal of Ecology]–>Russ. J. Ecol. 32, 343–351.
Berthon, V., Marchetto, A., Rimet, F., Dormia, E., Jenny, J.-P., Pignol, C., Perga, M.-E., 2013. Trophic history of French sub-Alpine lakes over the last ~150 years: phosphorus reconstruction and assessment of taphonomic biases. J. Limnol. 72 (3), 417–429.
Bertrand, J., Renon, J.P., Monnier, O., Ector, L., 2004. Relation 'diatomées épiphytes-bryophytes" dans les tourbières du Mont Lozère (France). Vie et Milieu 54 (2–3), 59–70.
Birks, H.J.B., 1995. Quantitative palaeoenvironmental reconstructions. In: Maddy, D., Brew, J.S. (Eds.), Statistical Modelling of Quaternary Science DataTechnical Guide Vol. 5. Quaternary Research Association, Cambridge, pp. 161–254.
Birks, H.J.B., 1998. Numerical tools in palaeolimnology-progress, potentialities, and problems. J. Paleolimnol. 20, 307–332.
Birks, H.J.B., Gordon, A.D., 1985. Numerical Methods in Quaternary Pollen Analysis. Academic Press, London.
Birks, H.J.B., Line, J.M., 1992. The use of rarefaction analysis for estimating palynological richness from Quaternary pollen-analytical data. The Holocene 2, 1–10.
Birks, H.J.B., Juggins, S., Line, J.M., 1990. Lake water chemistry reconstruction. In: Mason, B.J. (Ed.), The Surface Waters Acidification Programme. Cambridge University Press, Cambridge, pp. 301–313.
Birks, H.H., Jones, V.J., Brooks, S.J., Birks, H.J.B., Telford, R.J., Juggins, S., Peglar, S.M., 2012. From cold to cool in northernmost Norway: Lateglacial and early Holocene multiproxy environmental and climate reconstructions from Jansvatnet, Hammerfest. Quat. Sci. Rev. 22, 100–120.
Blaauw, M., 2010. Methods and code for 'classical' age-modelling of radiocarbon sequences. Quat. Geochronol. 5, 512–518.
Bouchard, G., Gajewski, K., Hamilton, P.B., 2004. Freshwater diatom biogeography in the Canadian Arctic Archipelago. J. Biogeogr. 31, 1955–1973.
Brodersen, K.P., Lindegaard, C., 1999. Mass occurrence and sporadic distribution of *Corynocera ambigua* Zetterstedt (Diptera, Chironomidae) in Danish lakes. Neo- and palaeolimnological records. Freshw. Biol. 42, 143–157.
Brodersen, K.P., Odgaard, B.V., Vestergaard, O., Anderson, N.J., 2001. Chironomid stratigraphy in the shallow and eutrophic Lake Sobygaard, Denmark: chironomid-macrophyte co-occurrence. Freshw. Biol. 46, 253–267.
Brodin, Y.W., 1986. The postglacial history of Lake Flarken, southern Sweden, interpreted from subfossil insect remains. Int. Rev. Gesamten Hydrobiol. 71, 371–432.
Brooks, S.J., 1996. Three thousand years of environmental history in a Cairngorms loch as revealed by analysis of non-biting midges (Insecta: Diptera: Chironomidae). Bot. J. Scotl. 48, 89–98.
Brooks, S.J., 2000. Late-glacial fossil midge stratigraphies (Insecta: Diptera: Chironomidae) from the Swiss Alps. Palaeogeogr. Palaeoclimatol. Palaeoecol. 159, 261–279.
Brooks, S.J., 2006. Fossil midges (Diptera: Chironomidae) as palaeoclimatic indicators for the Eurasian region. Quat. Sci. Rev. 25, 1894–1910.
Brooks, S.J., Birks, H.J.B., 2000. Chironomid-inferred late-glacial and early-Holocene mean July air temperature for Krakenes Lake, Western Norway. J. Paleolimnol. 23, 77–89.
Brooks, S.J., Birks, H.J.B., 2001. Chironomid-inferred air temperatures from Lateglacial and Holocene sites in north-west Europe: progress and problems. Quat. Sci. Rev. 20, 1723–1741.
Brooks, S.J., Langdon, P.G., 2014. Summer temperature gradients in northwest Europe during the Lateglacial to early Holocene transition (15-8 ka BP inferred from chironomid assemblages. Quat. Int. 341, 80–90.
Brooks, S.J., Bennion, H., Birks, H.J.B., 2001. Tracing lake trophic history with a chironomid–total phosphorus inference model. Freshw. Biol. 46, 513–533.
Brooks, S.J., Langdon, P.G., Heiri, O., 2007. The identification and use of Palaearctic Chironomidae larvae in palaeoecology. Technical Guide No 10. Quaternary Research Association, London.
Brooks, S.J., Davies, K.L., Mather, K.A., Matthews, I.P., Lowe, J.J., 2016. Chironomid-inferred summer temperatures for the Last Glacial–Interglacial Transition from a lake sediment sequence in Muir Park Reservoir, west-central Scotland. J. Quat. Sci. 31, 214–224.
Brundin, L., 1956. Die bodenfaunistischen Seentypen und ihre Anwendbarkeit auf die Sldhalbkugel. Zugleich eine Theorie der produktionsbiologischen Bedeutung der glazialen Erosion. 37. Report of the Institute of Freshwater Research, Drottningholm, pp. 186–235.
Brundin, L., 1958. The bottom faunistical lake type system and its application to the southern hemisphere. Moreover a theory of glacial erosion as a factor of productivity in lakes and oceans. Verh. Int. Ver. Theor. Angew. Limnol. 13, 288–297.
Buskens, R.F.M., 1987. The chironomid assemblages in shallow lentic waters differing in acidity, buffering capacity and trophic level in the Netherlands. Entomol. Scand. Suppl. 29, 217–224.
Cameron, N.G., Birks, H.J.B., Jones, V.J., Berge, F., Catalan, J., Flower, R.J., Garcia, J., Kawecka, B., Koinig, K.A., Marchetto, A., Sánchez-Castillo, P., Schmidt, R., Šiško, M., Solovieva, N., Štefková, E., Toro, M., 1999. Surface-sediment and epilithic diatom pH calibration sets for remote European mountain lakes (AL:PE project) and their comparison with the Surface Waters Acidification Programme (SWAP) calibration set. J. Paleolimnol. 22, 291–317.
Chen, J., Zhang, E., Brooks, S.J., Huang, X., Wang, H., Liu, J., Chen, F., 2013. Relationships between chironomids and water depth in Bosten Lake, Xinjiang, northwest China. J. Paleolimnol. 51, 313–323.
Colin, F., 1966. Le volcanisme de l'Aubrac (PhD Thesis, Clermond-ferrand).
Coope, G.R., 1986. Coleopteran analysis. In: Berglund, B.E. (Ed.), Handbook of Holocene Palaeoecology and Palaeohydrology. Wiley & Sons Ltd, Chichester, pp. 703–713.

Coope, G.R., Elias, S.A., 2000. The environment of Upper Palaeolithic (Magdalenian and Azilian) hunters at Hauterive Champréveyres, Neuchâtel, Switzerland, interpreted from coleopteran remains. J. Quat. Sci. 15, 157–175.

Coope, G.R., Lemdahl, G., 1995. Regional differences in the Lateglacial climate of northern Europe based on coleopteran analysis. J. Quat. Sci. 10, 391–395.

Coope, G.R., Lemdahl, G., Lowe, J.J., Walkling, A., 1998. Temperature gradients in northern Europe during the last glacial-Holocene transition (14-9 14C kyr BP) interpreted from coleopteran assemblages. J. Quat. Sci. 13, 419–433.

Core Team, R., 2012. R: A Language and Environment for Statistical Computing. R Foundation for Statistical Computing, Vienna.

Cranston, P., 2010. Online Chironomid Identification Key. (http://chirokey.skullisland.info/).

Danks, H.V., 1981. Arctic Arthropods: A Review of Systematics and Ecology With Particular Reference to the North American Fauna. Entomological Society of Canada, Ottawa.

Dixit, S.S., Cumming, C.F., Birks, H.J.B., Smol, J.P., Kingston, J.C., Uutala, A.J., Charles, D.F., Camburn, K.E., 1993. Diatom assemblages from Adirondack lakes (New York, USA) and the development of inference models for retrospective environmental assessment. J. Paleolimnol. 8, 27–47.

Enache, M., Prairie, Y.T., 2002. WA-PLS diatom-based pH, TP and DOC inference models from 42 lakes in the Abitibi clay belt area (Quebec, Canada). J. Paleolimnol. 27, 151–171.

Fallu, M.-A., Pienitz, R., 1999. Diatomées lacustres de Jamésie-Hudsonie (Québec) et modèle de reconstitution des concentrations de carbone organique dissous. Ecoscience 6 (4), 603–620.

Fallu, M.-A., Allaire, N., Pienitz, R., 2002. Distribution of freshwater diatoms in 64 Labrador (Canada) lakes: species-environment relationships along latitudinal gradients and reconstruction models for water colour and alkalinity. Can. J. Fish. Aquat. Sci. 59, 329–349.

Finkelstein, S.A., Gajewski, K., 2008. Responses of Fragilarioid-dominated diatom assemblages in a small Arctic lake to Holocene climatic changes, Russell Island, Nunavut, Canada. J. Paleolimnol. 40, 1079–1095.

Gachon, L., 1946. Les variétés régionales du climat dans le Massif central et le vrai Massif central climatique. Études rhodaniennes. 21 pp. 33–53.

Gaillard, M.J., Lemdahl, G., 1994. Lateglacial insect assemblages from Grand-Marais, south-western Switzerland-climatic implications and comparison with pollen and plant macrofossil data. Dissertationes botanicae 234, 287–308.

Gandouin, E., Maasri, A., Van Vliet-Lanoë, B., Franquet, E., 2006. Chironomid (Insecta: Diptera) assemblages from a gradient of lotic and lentic waterbodies in river floodplains of France: a methodological tool for palaeoecological applications. J. Paleolimnol. 35, 149–166.

Ginn, B.K., Cumming, B.F., Smol, J.P., 2007. Diatom-based environmental inferences and model comparisons from 494 northeastern North American lakes. J. Phycol. 43, 647–661.

Grimm, E.C., 1987. CONISS: a FORTRAN 77 program for stratigraphically constrained cluster analysis by the method of incremental sum of squares. Comput. Geosci. 13, 13–35.

Grimm, E.C., 1991. TILIA and TILIA GRAPH. Illinois State Museum, ISM Research and Collections Center, Springfield.

Hammer, Ø., Harper, D.A.T., Ryan, P.D., 2001. PAST: paleontological statistics software package for education and data analysis. Palaeontol. Electron. 4, 1–9.

Haworth, E.Y., 1976. Two late-glacial (late Devensian) diatom assemblage profiles from Northern Scotland. New Phytol. 77, 227–256.

Heiri, O., 2004. Within-lake variability of subfossil chironomid assemblages in shallow Norwegian lakes. J. Paleolimnol. 32, 67–84.

Heiri, O., Lotter, A.F., 2001. Effect of low count sums on quantitative environmental reconstructions: an example using subfossil chironomids. J. Paleolimnol. 26, 343–350.

Heiri, O., Millet, L., 2005. Reconstruction of Late Glacial summer temperatures from chironomid assemblages in Lac Lautrey (Jura, France). J. Quat. Sci. 20, 1–12.

Heiri, O., Lotter, A.F., Hausmann, S., Kienast, F., 2003. A chironomid-based Holocene summer air temperature reconstruction from the Swiss Alps. The Holocene 13, 477–484.

Heiri, O., Cremer, H., Engels, S., Hoek, W.Z., Peeters, W., Lotter, A.F., 2007a. Lateglacial summer temperatures in the Northwest European lowlands: a chironomid record from Hijkermeer, the Netherlands. Quat. Sci. Rev. 26, 2420–2437.

Heiri, O., Filippi, M.L., Lotter, A.F., 2007b. Lateglacial summer temperature in the Trentino area (Northern Italy) as reconstructed by fossil chironomid assemblages in Lago di Lavarone (1100 m a.s.l.). Studi Trentini di Scienze Naturali Acta Geologia 82, 299–308.

Heiri, O., Brooks, S.J., Birks, H.J.B., Lotter, A.F., 2011. A 274-lake calibration dataset and inference model for chironomid-based summer temperature reconstruction in Europe. Quat. Sci. Rev. 30, 3445–3456.

Heiri, O., Brooks, S.J., Renssen, H., Bedford, A., Hazekamp, M., Ilyashuk, B., Jeffers, E.S., Lang, B., Kirilova, E., Kuiper, S., Millet, L., Samartin, S., Toth, M., Verbruggen, F., Watson, J.E., van Asch, N., Lammertsma, E., Amon, L., Birks, H.H., Birks, H.J.B., Mortensen, M.F., Hoek, W.Z., Magyari, E., Munoz Sobrino, C., Seppä, H., Tinner, W., Tonkov, S., Veski, S., Lotter, A.F., 2014. Validation of climate model-inferred regional temperature change for late-glacial Europe. Nat. Commun. 5, 4914.

Henrichs, M.L., Walker, I.R., Mathewes, R.W., 2001. Chironomid-based paleosalinity records in southern British Columbia, Canada: a comparison of transfer functions. J. Paleolimnol. 26, 147–159.

Hickman, M., 1975. Studies on the epipelic diatom flora of some lakes in the southern Yukon Territory, Canada. Arch. Hydrobiol. 76, 420–448.

Hoek, W.Z., 2008. The last glacial-interglacial transition. Episodes 31, 226–229.

Hofmann, W., 1984. Stratigraphie subfossiler Cladocera (Crustacea) und Chironomidae (Diptera) in zwei Sedimentprofilen des Meerfelder Maares. Cour. Forschungsinstitut Senckenberg 65, 67–80.

Hofmann, W., 1986. Chironomid analysis. In: Berglund, B.E. (Ed.), Handbook of Holocene Palaeoecology and Palaeohydrology. Wiley & Sons Ltd, Chichester, pp. 715–727.

Ilyashuk, B., Gobet, E., Heiri, O., Lotter, A.F., van Leeuwen, J.F.N., van der Knaap, W.O., Ilyashuk, E., Oberli, F., Ammann, B., 2009. Lateglacial environmental and climatic changes at the Maloja Pass, Central Swiss Alps, as recorded by chironomids and pollen. Quat. Sci. Rev. 28, 1340–1350.

Isarin, R.F.B., Bohncke, S.J.P., 1999. Mean July temperatures during the younger Dryas in northern and Central Europe as inferred from climate indicator plant species. Quat. Res. 51, 158–173.

Joynt III, E.H., Wolfe, A.P., 2001. Paleoenvironmental inference models from sediment diatom assemblages in Baffin Island lakes (Nunavut, Canada) and reconstruction of summer water temperature. Can. J. Fish. Aquat. Sci. 58, 1222–1243.

Juggins, S., 2010. C2 Data Analysis. Version 1.6.5. University of Newcastle, Newcastle.

Juggins, S., 2013. Quantitative reconstructions in palaeolimnology: new paradigm or sick science? Quat. Sci. Rev. 64, 20–32.

Kesler, D.H., 1981. Grazing rate determination of *Corynoneura scutellata* Winnertz (Chironomidae: Diptera). Hydrobiologia 80, 63–66.

Kessler, J., Chambraud, A., 1986. La météo de la France. Tous les climats localité par localité. Editions J. C, Lattès, Paris (312 p).

Kingston, J.C., Birks, H.J.B., 1990. Dissolved organic carbon reconstructions from diatom assemblages in PIRLA project lakes, North America. Philos. Trans. R. Soc. Lond. B 327, 279–288.

Kingston, J.C., Lowe, R.L., Stoermer, E.F., Ladewski, T.B., 1983. Spatial and temporal distribution of benthic diatoms in northern Lake Michigan. Ecology 64, 1566–1580.

Klink, A.G., Moller Pillot, H.K.M., 2003. Chironomidae Larvae: Key to Higher Taxa and Species of the Lowlands of Northwestern Europe. World Biodiversity Database, Amsterdam.

Kocev, D., Naumoski, A., Mitreski, K., Krstić, S., Džeroski, S., 2010. Learning habitat models for the diatom community in Lake Prespa. Ecol. Model. 221, 330–337.

Korhola, A., Vasko, K., Toivonen, H.T.T., Olander, H., 2002. Holocene temperature changes in northern Fennoscandia reconstructed from chironomids using Bayesian modelling. Quat. Sci. Rev. 21, 1841–1860.

Korsman, T., Birks, H.J.B., 1996. Diatom-based water chemistry reconstructions from northern Sweden: a comparison of reconstruction techniques. J. Paleolimnol. 15, 65–77.

Krammer, K., Lange-Bertalot, H., Mollenhauer, D., 1986. Bacillariophyceae. 1. Teil: Naviculaceae. In: Ettl, H., Gerloff, J., Heynig, H. (Eds.), Süsswasserflora von Mitteleuropa, Band 2/1. Gustav Fischer Verlag, Stuttgart (876 pp).

Krammer, K., Lange-Bertalot, H., 1988. Bacillariophyceae. 2. Teil: Bacillariaceae, Epithemiaceae, Surirellaceae. In: Ettl, H., Gerloff, J., Heynig, H., Mollenhauer, D. (Eds.), Süsswasserflora von Mitteleuropa, Band 2/2. Gustav Fischer Verlag, Stuttgart (596 pp).

Krammer, K., Lange-Bertalot, H., 1991a. Bacillariophyceae. 3. Teil: Centrales, Fragilariaceae, Eunotiaceae. In: Ettl, H., Gerloff, J., Heynig, H., Mollenhauer, D. (Eds.), Süsswasserflora von Mitteleuropa, Band 2/3. Gustav Fischer Verlag, Stuttgart (576 pp).

Krammer, K., Lange-Bertalot, H., 1991b. Bacillariophyceae. 4. Teil: Achnanthaceae, Kritische Ergänzungen zu *Navicula* (Lineolatae) und *Gomphonema*, Gesamtliteraturverzeichnis Teil 1-4. In: Ettl, H., Gärtner, G., Gerloff, J., Heynig, H., Mollenhauer, D. (Eds.), Süsswasserflora von Mitteleuropa, Band 2/4. Gustav Fischer, Stuttgart (437 pp.).

Laing, T.E., Smol, J.P., 2000. Factors influencing diatom distributions in circumpolar treeline lakes of northern Russia. J. Phycol. 36, 1035–1048.

Lang, B., Brooks, S.J., Bedford, A., Jones, R.T., Birks, H.J.B., Marshall, J.D., 2010. Regional consistency in Lateglacial chironomid-inferred temperatures from five sites in north-west England. Quat. Sci. Rev. 29, 1528–1538.

Larocque, I., 2001. How many chironomid head capsules is enough? A statistical approach to determine sample size for paleoclimatic reconstruction. Palaeogeogr. Palaeoclimatol. Palaeoecol. 172, 133–142.

Larocque, I., Bigler, C., 2004. Similarities and discrepancies between chironomid- and diatom-inferred temperature reconstructions through the Holocene at Lake 850, northern Sweden. Quat. Int. 122, 109–121.

Larocque, I., Finsinger, W., 2008. Late-glacial chironomid-based temperature reconstructions for Lago Piccolo di Avigliana in the southwestern Alps (Italy). Palaeogeogr. Palaeoclimatol. Palaeoecol. 257, 207–223.

Larocque, I., Hall, R.I., 2004. Holocene temperature estimates and chironomid community composition in the Abisko Valley, northern Sweden. Quat. Sci. Rev. 23, 2453–2465.

Larocque, I., Hall, R.I., Grahn, E., 2001. Chironomids as indicators of climate change: a 100-lake training set from a subarctic region of northern Sweden (Lapland). J. Paleolimnol. 26, 307–322.

Larocque-Tobler, I., Heiri, O., Wehrli, M., 2010. Late Glacial and Holocene temperature changes at Egelsee, Switzerland, reconstructed using subfossil chironomids. J. Paleolimnol. 43, 649–666.

Lotter, A.F., Bigler, C., 2000. Do diatoms in the Swiss Alps reflect the length of ice-cover? Aquat. Sci. 62, 125–141.

Lotter, A.F., Juggins, S., 1991. ZONE. Unpublished computer software.

Lotter, A.F., Birks, H.J.B., Hofmann, W., Marchetto, A., 1997. Modern diatom, cladocera, chironomid and chrysophyte cyst assemblages as quantitative indicators for the reconstruction of past environmental conditions in the Alps. I. Climate. J. Paleolimnol. 19, 395–420.

Lotter, A.F., Heiri, O., Brooks, S.J., van Leeuwen, J.F.N., Eicher, U., Ammann, B., 2012. Rapid summer temperature changes during termination 1a: high-resolution multiproxy climate reconstructions from Gerzensee (Switzerland). Quat. Sci. Rev. 36, 103–113.

Lowe, J.J., Rasmussen, S.O., Björck, S., Hoek, W.Z., Steffensen, J.P., Walker, M.J.C., Yu, Z., INTIMATE group, 2008. Precise dating and correlation of events in the North Atlantic region during the Last Termination: a revised protocol recommended by the INTIMATE group. Quat. Sci. Rev. 27, 6–17.

Météo France, 2003. www.meteofrance.com.

Millet, L., Rius, D., Galop, D., Heiri, O., Brooks, S.J., 2012. Chironomid-based reconstruction of Lateglacial summer temperatures from the Ech palaeolake record (French western Pyrenees). Palaeogeogr. Palaeoclimatol. Palaeoecol. 315-316, 86–99.

Moller Pillot, H.K.M., Buskens, R.F.M., 1990. De larven der Nederlandse Chironomidae (Diptera) Deel C: Autoekologie en verspreiding. Nederlandse Faunistische Mededelingen. 1 pp. 1–277.

Moreno, A., Svensson, A., Brooks, S.J., Connor, S., Engels, S., Fletcher, W., Genty, D., Heiri, O., Labuhn, I., Perşoiu, A., Peyron, O., Sadori, L., Valero-Garcés, B., Wulf, S., Zanchetta, G.,

2014. A compilation of Western European terrestrial records 60–8 ka BP: towards an understanding of latitudinal climatic gradients. Quat. Sci. Rev. 106, 167–185.
Mousavi, K., 2002. Boreal chironomid communities and their relations to environmental factors - the impact of lake depth, size and acidity. Boreal Environ. Res. 7, 63–75.
Muñoz Sobrino, C., Heiri, O., Hazekamp, M., van der Velden, D., Kirilova, E.P., Garcia-Moreiras, I., 2013. New data on the Lateglacial period of SW Europe: a high resolution multiproxy record from Laguna de la Roya (NW Iberia). Quat. Sci. Rev. 80, 58–77.
Nozeran, R., 1953. Aperçu sur lemilieu physique et la flore du Massif de l'Aubrac. Bulletin de la Société Botanique de France. 100 pp. 8–21.
Olander, H., Birks, H.J.B., Korhola, A., Blom, T., 1999. An expanded calibration model for inferring lake water and air temperatures from fossil chironomid assemblages in northern Fennoscandia. The Holocene 9, 279–294.
Padisàk, J., Crossetti, L.O., Naselli-Flores, L., 2009. Use and misuse in the application of the phytoplankton functional classification: a critical review with updates. Hydrobiologia 621, 1–19.
Pavlov, A., Levkov, Z., 2013. Diversity and distribution of taxa in the genus *Eunotia* Ehrenberg (Bacillariophyta) in Macedonia. Phytotaxa 86 (1), 1–117.
Peyron, O., Bégeot, C., Brewer, S., Heiri, O., Magny, M., Millet, L., Ruffaldi, P., Van Campo, E., Yu, G., 2005. Late-Glacial climatic changes in Eastern France (Lake Lautrey) from pollen, lake-levels, and chironomids. Quat. Res. 64, 197–211.
Podritske, B., Gajewski, K., 2007. Diatom community response to multiple scales of Holocene climate variability in a small lake on Victoria Island, NWT, Canada. Quat. Sci. Rev. 26, 3179–3196.
Poizat, M., Rousset, C., 1975. Les calottes de glace quaternaires des Monts d'Aubrac (Massif Central, France): caractéristiques. Contexte Paléoclimatique. Revue de Géographie Physique et de Géologie Dynamique. 12 pp. 171–190.
Ponel, P., Coope, G.R., 1990. Lateglacial and early Flandrian Coleoptera from La Taphanel, Massif Central, France: climatic and ecological implications. J. Quat. Sci. 5, 235–249.
Ponel, P., Coope, G.R., Antoine, P., Limondin-Lozouet, N., Leroyer, C., Munaut, A.V., Pastre, J.F., Guiter, F., 2005. Lateglacial palaeoenvironments and palaeoclimates from Conty and Houdancourt, northern France, reconstructed from Beetle remains. Quat. Sci. Rev. 24, 2449–2465.
Quinlan, R., Smol, J.P., 2001. Setting minimum head capsule abundance and taxa deletion criteria in chironomid-based inference models. J. Paleolimnol. 26, 327–342.
Reimer, P.J., Bard, E., Bayliss, A., Beck, J.W., Blackwell, P.G., Bronk Ramsey, C., Buck, C.E., Edwards, R.L., Friedrich, M., Grootes, P.M., Guilderson, T.P., Haflidason, H., Hajdas, I., Hatté, C., Heaton, T.J., Hoffmann, D.L., Hogg, A.G., Hughen, K.A., Kaiser, K.F., Kromer, B., Manning, S.W., Niu, M., Reimer, R.W., Richards, D.A., Scott, E.M., Southon, J.R., Turney, C.S.M., van der Plicht, J., 2013. IntCal13 and Marine13 radiocarbon age calibration curves, 0–50,000 years cal BP. Radiocarbon 55, 1869–1887.
Renssen, H., Vandenberghe, J., 2003. Investigation of the relationship between permafrost distribution in NW Europe and extensive winter sea-ice cover in the North Atlantic Ocean during the cold phases of the Last Glaciation. Quat. Sci. Rev. 22, 209–223.
Renssen, H., Seppä, H., Heiri, O., Roche, D.M., Goose, H., Fichedet, 2009. The spatial and temporal complexity of the Holocene thermal maximum. Nat. Geosci. 2, 411–414.
Rieradevall, M., Brooks, S.J., 2001. An identification guide to subfossil Tanypodinae larvae (Insecta: Diptera: Chironomidae) based on cephalic setation. J. Paleolimnol. 25, 81–99.
Rosén, P., Hall, R.I., Korsman, T., Renberg, I., 2000. Diatom transfer-functions for quantifying past air temperature, pH and total organic carbon concentration from lakes in northern Sweden. J. Paleolimnol. 24, 109–123.
Round, F.E., Crawford, R.M., Mann, D.G., 1990. The Diatoms. Biology and Morphology of the Genera. Cambridge University Press, Cambridge (747 pp.).
Schmid, P.E., 1993. A key to the larval chironomidae and there instars from Austrian Danube region streams and rivers. Part 1. Diamesinae, Prodiamesinae and Orthocladiinae. Federal Institute for Water Quality, Vienna.
Schmidt, R., Kamenik, C., Lange-Bertalot, H., Klee, R., 2004. *Fragilaria* and *Staurosira* (Bacillariophyceae) from sediment surfaces of 40 lakes in the Austrian Alps in relation to environmental variables, and their potential for palaeoclimatology. J. Paleolimnol. 63, 171–189.
Smol, J.P., 1985. The ratio of diatom frustules to chrysophycean statospores: a useful paleolimnological index. Hydrobiologia 123, 199–208.
Stevenson, A.C., Juggins, S., Birks, H.J.B., Anderson, D.S., Anderson, N.J., Battarbee, R.W., Berge, F., Davis, R.B., Flower, R.J., Haworth, E.Y., Jones, V.J., Kingston, J.C., Kreiser, A.M., Line, J.M., Munro, M.A.R., Renberg, I., 1991. The Surface Water Acidification Project Palaeolimnology Programme: Modern Diatom/Lake-Water Chemistry Data-Set. Ensis Ltd, London (86 pp.).
Stoermer, E.F., Smol, J.P., 1999. The Diatoms: Applications for the Environmental and Earth Sciences. Cambridge University Press, Cambridge, UK (469 pp.).
Telford, R.J., Birks, H.J.B., 2011. A novel method for assessing the statistical significance of quantitative reconstructions inferred from biotic assemblages. Quat. Sci. Rev. 30, 1272–1278.
ter Braak, C.J.F., Šmilauer, P., 2002. CANOCO for Windows Version 4.5. Biometrics. Plant Research International, Wageningen, The Netherlands.
Velle, G., Brooks, S.J., Birks, H.J.B., Willassen, E., 2005. Chironomids as a tool for inferring Holocene climate: an assessment based on six sites in southern Scandinavia. Quat. Sci. Rev. 24, 1429–1462.
Walker, I.R., MacDonald, G.M., 1995. Distributions of Chironomidae (Insecta: Diptera) and other freshwater midges with respect to treeline, Northwest Territories, Canada. Arct. Antarct. Alp. Res. 27, 258–263.
Watson, J.E., Brooks, S.J., Whitehouse, N.J., Reimer, P.J., Birks, H.J.B., Turney, C., 2010. Chironomid-inferred late-glacial summer air temperatures from Lough Nadourcan, Co. Donegal, Ireland. J. Quat. Sci. 25, 1200–1210.
Wetzel, R.G., 2001. Limnology. Lake and River Ecosystems. Third edition. Academic Press, San Diego (1006 pp.).
Wiederholm, T., 1983. Chironomidae of the Holarctic region. Keys and diagnoses. Part I: larvae. Entomol. Scand. Suppl. 19, 1–417.
Witkowski, A., Lange-Bertalot, H., Metzeltin, D., 1995. The diatom species *Fragilaria martyi* (Heribaud) Lange-Bertalot, identity and ecology. Arch. Protistenkd. 146, 281–292.